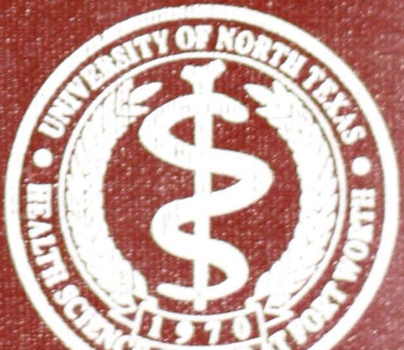
UNIVERSITY OF NORTH TEXAS
HEALTH SCIENCE CENTER AT FORT WORTH
1970

UNTHSC - FW
M02E17

LE[illegible] LIBRARY
[illegible] Center
[illegible] Camp [illegible]ie Blvd.
Ft. Worth, Texas 76107-2699

Gibson, Grant E., Isotope Partitioning and Initial Velocity Studies with 6-Phosphofructo-1-kinase from *Ascaris suum*. Doctor of Philosophy (Biomedical Sciences), May, 1996, 91 pages, 2 tables, 18 figures, 2 schemes, 1 reaction, 2 mechanisms, 1 diagram, bibliography, 61 titles.

The native *Ascaris suum* 6-phosphofructo-1-kinase (nPFK) and a chemically modified form (dPFK) which is desensitized to allosteric behavior have been studied using isotope partitioning and initial velocity techniques to determine the kinetic mechanism as well as the effects of fructose 2,6-bisphosphate ($F26P_2$) and $Mg^{2+}$ on the mechanism. At 8 mM $Mg^{2+}$, complete trapping ($P^*_{max} \approx 100\%$) of the E:MgATP* complex as fructose 1-($^{32}P$),6-bisphosphate for both enzyme forms is consistent with the previously proposed steady-state ordered mechanism (Rao, G.S.J., Harris, B.G., and Cook, P.F. (1987) *J. Biol. Chem.* **262**, 14074-14079) with MgATP binding before fructose 6-phosphate (F6P). A saturating amount of $F26P_2$ causes no change in the trapping parameters for nPFK but causes a decrease in both $P^*_{max}$ and $K'_{F6P}$ for dPFK. The partial trapping of E:MgATP* in the presence of $F26P_2$ for dPFK at high $Mg^{2+}$ suggests that the activator changes the kinetic mechanism from an ordered to a random binding of substrates. Initial velocity studies at 8 mM $Mg^{2+}$ confirm the change in mechanism. Uncompetitive inhibition by arabinose 5-phosphate (Ara5P), a dead-end inhibitory analog of F6P, versus MgATP for nPFK in the absence and presence of $F26P_2$ is consistent with an ordered mechanism with MgATP adding to enzyme prior to F6P. An uncompetitive pattern is also obtained with dPFK for Ara5P versus MgATP in the absence of $F26P_2$, but the pattern becomes noncompetitive in the presence of $F26P_2$, consistent with a change to a random mechanism. No trapping of the dPFK:($^{14}C$)F6P complex could be detected at 8 mM $Mg^{2+}$, indicating either that the dPFK:$^{14}C$-F6P complex does not form or that the off-rate

for F6P from enzyme is much faster than the net rate constant for formation of the first product, FBP. Initial velocity data indicate that a second $Mg^{2+}$ ion in addition to the one bound in MgATP is an essential activator of *Ascaris suum* PFK which decreases the off-rate for MgATP. $K_{act}$ for $Mg^{2+}$ is estimated to be 0.47 ± 0.08 mM. Isotope partitioning data at 0.1 mM $Mg^{2+}$ indicate that dPFK is able to trap only 20% of the E:MgATP* both in the presence and absence of $F26P_2$, consistent with a faster off-rate for MgATP at low $Mg^{2+}$ than at high $Mg^{2+}$. Partial trapping of MgATP* at low $Mg^{2+}$ again suggests a random binding of substrates. Noncompetitive Ara5P inhibition versus MgATP at low $Mg^{2+}$ confirms the random mechanism. An active site role both in binding MgATP and in facilitating catalysis is proposed for the second $Mg^{2+}$. Furthermore, calculations from the isotope partitioning and initial velocity data as well as changes that are seen in the circular dichroic spectra for both nPFK and dPFK indicate that an enzyme structural isomerization occurs upon binding MgATP.

# ISOTOPE PARTITIONING AND INITIAL VELOCITY STUDIES WITH 6-PHOSPHOFRUCTO-1-KINASE FROM *Ascaris suum*

Grant E. Gibson, B.S.

APPROVED:

Major Professor

Major Professor

Committee Member

Committee Member

Committee Member

Mark E. Hart

Committee Member

Chair, Department of Biochemistry

Thomas Yorio

Dean, Graduate School of Biomedical Sciences

# ISOTOPE PARTITIONING AND INITIAL VELOCITY STUDIES WITH 6-PHOSPHOFRUCTO-1-KINASE FROM *Ascaris suum*

DISSERTATION

Presented to the Graduate Council of the
Graduate School of Biomedical Sciences
University of North Texas Health Science Center at Fort Worth
in Partial Fulfillment of the Requirements
For the Degree of

DOCTOR OF PHILOSOPHY

By

Grant E. Gibson, B.S.
Fort Worth, Texas
June, 1996

# TABLE OF CONTENTS

Chapter Page

LIST OF FIGURES....v

LIST OF TABLES..vii

LIST OF ILLUSTRATIONS.viii

LIST OF ABBREVIATIONS.ix

I. INTRODUCTION...1

Regulation of PFK.4

Desensitized *Ascaris suum* PFK...6

Chemical Mechanism of *Ascaris suum* PFK...7

Kinetic Mechanism of *Ascaris suum* PFK...6

Isotope partitioning..10

II. METHODS.15

Chemicals..15

Purification of *Ascaris suum* PFK..15

Chemical modification of native PFK..15

Initial velocity studies..16

$Mg^{2+}$-chelate correction..17

Circular dichroism spectral measurements..18

Isotope partitioning studies..18

Data analysis.21

III. ISOTOPE PARTITIONING AND INITIAL VELOCITY STUDIES WITH PHOSPHOFRUCTOKINASE AT HIGH $[Mg^{2+}]_{free}$..23

$K_D$ Determination.24

Isotope partitioning of nPFK:MgATP* ± $F26P_2$ ..30

Isotope partitioning of dPFK:MgATP* ± $F26P_2$ ..30

Isotope partitioning of dPFK:[$^{14}C$]F6P ..30

Initial velocity studies ..38

IV. ISOTOPE PARTITIONING AND INITIAL VELOCITY STUDIES WITH PHOSPHOFRUCTOKINASE AT VARIED $[Mg^{2+}]_{free}$ ..45

Initial velocity studies at varied $Mg^{2+}$ ..45

$K_D$ Determination ..57

Isotope partitioning of dPFK:MgATP* ± $F26P_2$ at low $Mg^{2+}$ ..57

Arabinose 5-phosphate inhibition ..63

VI. DISCUSSION ..68

Isotope partitioning at high $Mg^{2+}$ - $F26P_2$ ..68

Isotope partitioning at high $Mg^{2+}$ + $F26P_2$ ..70

Initial velocity studies at high $Mg^{2+}$ ..72

Initial velocity studies at varied $Mg^{2+}$ ..74

Isotope partitioning at low $Mg^{2+}$ ..75

Structural isomerization of the E:MgATP complex ..76

Effects of $F26P_2$ on the PFK-catalyzed reaction ..78

Effects of $Mg^{2+}$ on the PFK-catalyzed reaction ..82

Conclusions ..85

VIII. REFERENCES ..87

## LIST OF FIGURES

FIGURE 1. Circular Dichroic Spectra for *Ascaris suum* PFK in the Absence and Presence of MgATP........26

FIGURE 2. $K_D$ Determination for the PFK:MgATP Complex........28

FIGURE 3. Isotope Trapping of the E:MgATP* Complex with *Ascaris suum* nPFK (pH 8.0) in the Absence of $F26P_2$........31

FIGURE 4. Isotope Trapping of the E:MgATP* Complex with *Ascaris suum* nPFK (pH 8.0) in the Presence of $F26P_2$........33

FIGURE 5. Isotope Trapping of the E:MgATP* Complex with dPFK (pH 6.8) in the Absence of $F26P_2$........35

FIGURE 6. Isotope Trapping of the E:MgATP* Complex with dPFK (pH 6.8) in the Presence of $F26P_2$........37

FIGURE 7. Typical Initial Velocity Pattern for *Ascaris suum* PFK........39

FIGURE 8. Arabinose 5-Phosphate Inhibition Pattern for nPFK (pH 8.0) in the Presence of $F26P_2$........41

FIGURE 9. Arabinose 5-Phosphate Inhibition Pattern for nPFK (pH 8.0) in the Presence of $F26P_2$........43

FIGURE 10. $Mg^{2+}$ Activation Plot for dPFK at Non-saturating Substrate Concentration........47

FIGURE 11. Initial Velocity Pattern for dPFK at 0.1 mM $Mg^{2+}$ in the Absence of $F26P_2$........49

FIGURE 12. Initial Velocity Pattern for dPFK at 2.0 mM $Mg^{2+}$ in the Absence of $F26P_2$........51

FIGURE 13. $K_{act}$ Determination for $Mg^{2+}$ Activation of dPFK........53

FIGURE 14. $Mg^{2+}$ Versus MgATP Pattern at a Saturating Concentration of F6P........55

FIGURE 15. Initial Velocity Pattern for dPFK at 0.1 mM $Mg^{2+}$ in the Presence of $F26P_2$ ..59

FIGURE 16. Isotope Trapping of the dPFK:MgATP* Complex at Low and High $Mg^{2+}$ in the Absence and Presence of $F26P_2$ ..61

FIGURE 17. Arabinose 5-Phosphate Inhibition of dPFK at 0.1 mM $Mg^{2+}$ in the Absence of $F26P_2$ ..64

FIGURE 18. Arabinose 5-Phosphate Inhibition of dPFK at 0.1 mM $Mg^{2+}$ in the Presence of $F26P_2$ ..66

# LIST OF TABLES

TABLE 1. Summary of Data from Isotope Partitioning of E:MgATP* with *Ascaris suum* PFK at High $Mg^{2+}$ ..25

TABLE 2. Summary of Data from Isotope Partitioning of dPFK:MgATP* at Low and High $Mg^{2+}$ ..58

# LIST OF ILLUSTRATIONS

**REACTION I.** The PFK Reaction...........................................................2

**MECHANISM I.** Acid-Base Mechanism for *Ascaris suum* PFK........................ ...8

**DIAGRAM I.** A Typical Isotope Partitioning Experiment...................................11

**SCHEME I.** Steps in the Substrate Trapping of MgATP* with PFK.......................71

**SCHEME II.** Kinetic Mechanism of *Ascaris suum* PFK.................................. ..77

**MECHANISM II.** $Mg^{2+}$ Activation Mechanism of *Ascaris suum* PFK................. ..83

# LIST OF ABBREVIATIONS

Ara5P, arabinose 5-phosphate

BME, β-mercaptoethanol

DEPC, diethyl pyrocarbonate

F6P, fructose 6-phosphate; FBP, fructose 1,6-bisphosphate

$F26P_2$, fructose 2,6-bisphosphate

MgATP*, Mg[$\gamma$-$^{32}$P]ATP

oATP, periodate-oxidized ATP

PFK, phosphofructokinase, with the leading consonants n, d, and o indicating the native, desensitized, and oATP-modified forms, respectively.

# CHAPTER I

# INTRODUCTION

Phosphofructokinase (PFK) catalyzes the phosphoryl transfer of the $\gamma$-phosphate of MgATP to the C1 hydroxyl of fructose 6-phosphate to give fructose 1,6-bisphosphate (Reaction I). Phosphofructokinase and the metabolic pathway to which it belongs, glycolysis, are common to many life forms including both aerobic and anaerobic organisms. Glycolysis provides only the first steps in the complete oxidation of glucose in aerobic organisms, but the glycolytic pathway is able to provide most or all of the metabolic energy necessary in anaerobic organisms. The PFK reaction is sufficiently exergonic so that it is essentially irreversible *in vivo*. As such, the reaction is the committed step in glycolysis and is the key regulatory step of the glycolytic pathway.

Glycolysis is particularly important in the parasitic helminth *Ascaris suum*, which has been shown to use anaerobic carbohydrate metabolism as its sole source of energy (Saz, 1971). *A. suum* is a mammalian parasite which is most commonly found in pigs. The adult *A. suum* worm lives in the small intestine, where it feeds upon the chyme of the host. Copulation occurs in the small intestine, and fertilized eggs pass out of the intestine in the feces. Eggs are able to develop in moist soil in the presence of oxygen. Active larvae undergo a molt within the eggshell, at which time the egg becomes infective. When infective eggs are swallowed, the larvae hatch in the host's small intestine and burrow through the intestinal lining. Within about 2 weeks, the larvae are transported via the circulatory system to the lungs of the host, where they rupture the capillaries in which they are carried. Two more molts occur during the migration of the

## REACTION I.

### The PFK Reaction.

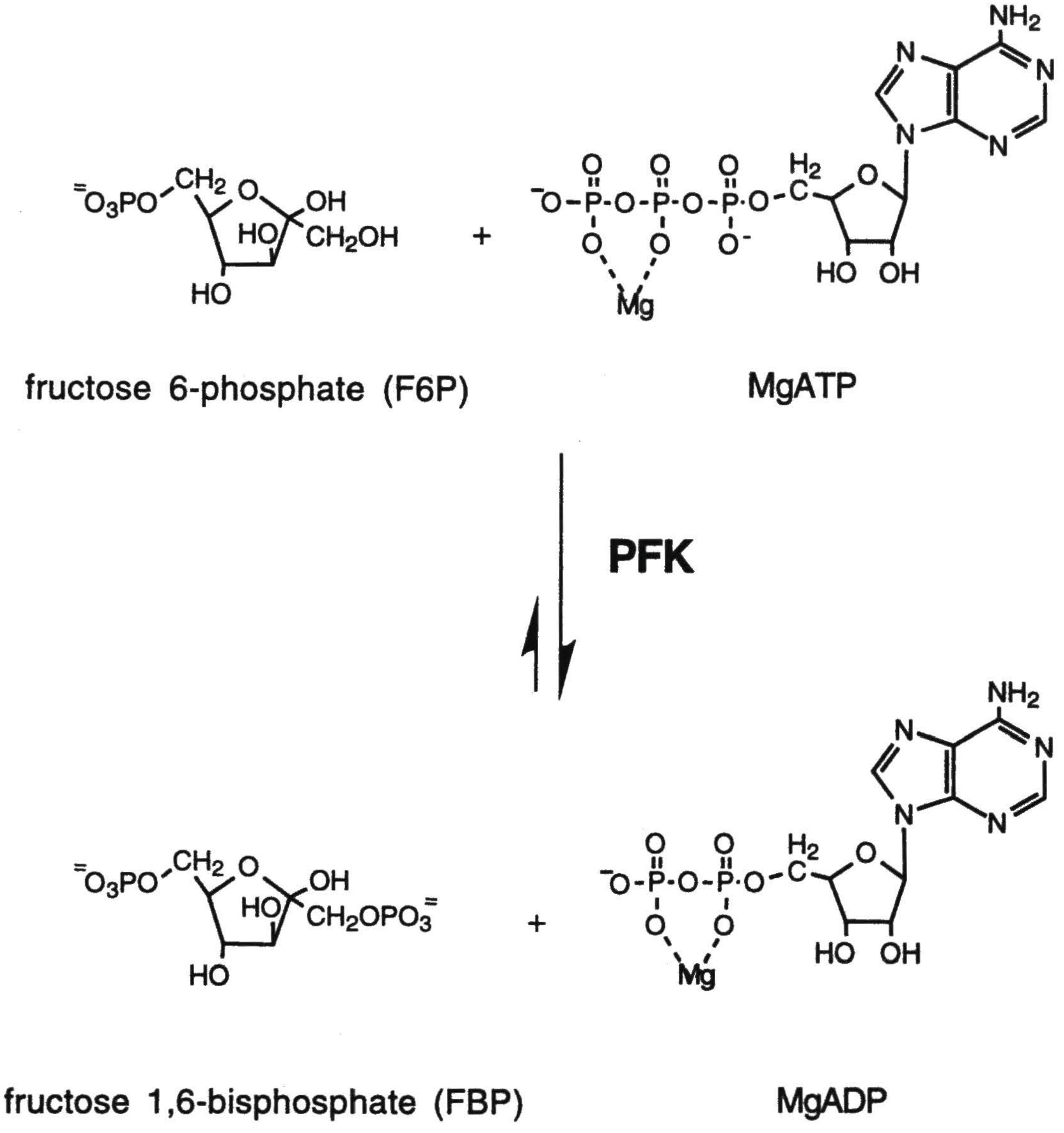
fructose 6-phosphate (F6P)
MgATP
PFK
fructose 1,6-bisphosphate (FBP)
MgADP

larvae from the intestine to the lungs. The larvae are coughed up from the lungs and swallowed by the host. Entering the small intestine once again, the *A. suum* larvae undergo a final molt, after which they are able to survive in the small intestine and develop to maturity (Cheng, 1986).

Although the developing fertilized egg requires oxygen for growth, the adult *A. suum* parasite is able to survive in the completely anaerobic environment of the small intestine. In addition, the adult worm, which has no hold-fast organs such as hooks or suckers, must constantly swim against the peristaltic motion of the intestine. Thus, a large amount of anaerobic energy is required for the survival of the worm. Having no TCA cycle and no fatty acid or amino acid metabolism (Saz, 1971; Payne *et al.*, 1979), the adult *A. suum* worm relies solely on anaerobic carbohydrate metabolism. The parasite has been shown to store large amounts of glycogen in its muscle tissue during a feeding cycle of the host (Donahue *et al.*, 1981). The glycogen provides glucose residues which can be broken down through glycolysis and further metabolic reactions.

The ascarid glycolytic pathway differs from that of most other organisms in that phosphoenol-pyruvate (PEP) is not converted to pyruvate, but instead is converted to oxaloacetate by a cytoplasmic PEP-carboxykinase. Oxaloacetate is then converted to malate by a cytoplasmic malate dehydrogenase. Malate enters the mitochondrion where it undergoes a dismutation, ultimately giving volatile fatty acids as end products. The mitochondrial reactions have been shown to give at least 1 equivalent of ATP for 2 equivalents of malate (Saz and Lescure, 1969; Saz, 1971; Payne *et al.*, 1979). Thus, glycolysis plays a critical role in the overall energy metabolism of the adult *A. suum* worm. The glycolytic enzymes from the muscle of *A. suum* are structurally and catalytically similar to those of the mammalian hosts, but the enzymes from the parasite appear to be specialized for carbohydrate-based metabolism (Supowit and Harris, 1976).

As in most organisms, PFK from *A. suum* catalyzes the rate-limiting step in glycolysis, providing an ideal point for regulation.

*Regulation of PFK.* Phosphofructokinase is one of the most highly regulated enzymes that has been studied. Much of the research that has been done on PFK has been directed toward an understanding of the allosteric behavior of the enzyme. The activity of PFK from various organisms is influenced by a number of effectors. In general, bacterial PFK is affected by only a few metabolites, while PFK from higher organisms has many allosteric effectors (Uyeda, 1970). Although the allosteric properties of PFK vary from species to species, several general characteristics have been identified, including inhibition by ATP and/or citrate, activation by AMP or ADP, and positive cooperativity of F6P binding. The physiological significance of the influence of the adenosine nucleotides or citrate is easily seen, since glycolysis serves to generate ATP in anaerobic cells and can further provide oxidizable intermediates, such as citrate, for mitochondria in aerobic cells. A high level of ATP or citrate in the cell would indicate the need to slow down glycolysis by feedback-inhibiting PFK, while a high level of AMP or ADP in the cell would indicate the need to speed up glycolysis by activating PFK.

*A. suum* PFK exhibits strong inhibition by ATP, as well as hysteresis in reaction time courses, positive cooperativity of F6P binding, activation by many small ion effectors, and activation by AMP and fructose 2,6-bisphosphate ($F26P_2$; Payne *et al.*, 1991). $F26P_2$ is the most potent activator of both mammalian PFK (Van Shaftingen, 1987; Claus *et al.*, 1984; Uyeda *et al.*, 1982) and parasite PFK (Kamemoto & Mansour, 1986; Srinivasan *et al.*, 1990). Data for the *Ascaris* enzyme indicate that both $F26P_2$ and AMP increase the affinity of the enzyme for F6P (Payne *et al.*, 1991). The sensitive nature of PFK to effectors has led researchers to carry out initial velocity studies at pH 7.5 - 8.0, where the allosteric behavior is minimized (Uyeda, 1979). *Ascaris suum* PFK at pH 8 has been shown to have essentially no inhibition by ATP and no

cooperativity of F6P binding (Rao *et al.*, 1987b). However, the effectors $F26P_2$ and AMP still activate the enzyme at pH 8 (Rao *et al.*, 1991a). Structural studies with the *Ascaris* enzyme using circular dichroism have indicated that the structural changes that occur upon increasing the pH from 6.8 to 8.0 are distinct from those which occur in the presence of $F26P_2$ or AMP (Rao *et al.*, 1991a; and Rao *et al.*, 1995).

In addition to the above-mentioned allosteric properties, phosphorylation plays an important role in the regulation of PFK in *Ascaris suum* (Hofer *et al.*, 1982). The enzyme from the muscle of the parasite can be isolated with 1 to 2 phosphates per subunit of enzyme (Starling *et al.*, 1982). Phosphorylation has been shown to stimulate the activity of PFK from *A. suum*, and also from two other helminths, *Fasciola hepatica* (Kamemoto & Mansour, 1986; Kamemoto *et al.*, 1987) and *Dirofilaria immitis* (Srinivasan *et al.*, 1988). The activation of the *A. suum* enzyme is thought to be caused by decreasing the dissociation constant for F6P, causing a change in the order of binding of substrates (Payne *et al.*, 1991). PFK purified from *A. suum* is capable of being phosphorylated both by bovine cAMP-dependent protein kinase and by a protein kinase isolated from *A. suum* muscle. Phosphorylation occurs at a specific serine residue and the sequence of the phosphorylation site is known (Kulkarni *et al.*, 1987). The Michaelis constant for PFK as a substrate of the *A. suum* muscle protein kinase is similar to the estimated concentration of PFK in the cell (Starling *et al.*, 1982), suggesting that the PFK is a physiological substrate for the protein kinase (Thalhofer *et al.*, 1988).

Further evidence for phosphorylation as a means of metabolic regulation in *A. suum* comes from the study of the effect of the putative hormone serotonin on muscle tissue from this organism. Serotonin-perfused *A. suum* muscle exhibits an increase in cAMP, activation of both glycogen phosphorylase and protein kinase activities, and an inactivation of glycogen synthase activity (Donahue *et al.*, 1983). Serotonin-induced

conformer, dPFK, a chemically-derived less active conformer, oPFK, has also been generated using periodate-oxidized ATP (oATP; Rao *et al.*, 1991b). The authors showed that the ATP analog, oATP, modifies the native enzyme at a ratio of 2 mol/subunit, giving an enzyme form which has only 10% of the native enzyme activity. Modification by oATP was further shown to result from the modification of an allosteric site lysine (pK 8.4) while the catalytic site remains intact. Thus, the activated dPFK is prepared in the presence of saturating F6P, and the less active oPFK is prepared in the presence of a saturating amount of an ATP analog, supporting a theory that F6P stabilizes a more active conformation and ATP stabilizes a less active conformation (Cook *et al.*, 1987).

*Chemical Mechanism of Ascaris suum PFK.* The effects of pH on the dPFK-catalyzed reaction and on the $F26P_2$ activation of the enzyme have recently been studied (Payne *et al.*, 1995). pH studies are not easily carried out and interpreted with native PFK because of the many pH-dependent allosteric changes that occur. Data obtained by Payne *et al.* (1995) allowed the authors to propose an acid/base mechanism for the *A. suum* PFK (Mechanism I). Briefly, an enzyme general base (pK 7.0) accepts a proton from the 1-hydroxyl of F6P concomitant with attack on the $\gamma$-phosphate of MgATP. A second enzyme group with a pK of 8.9 must be protonated and has been proposed to be involved in neutralizing the negative charge on MgATP to facilitate the nucleophilic attack by F6P. The authors further showed that V and $V/K_{MgATP}$ are pH-independent and are not affected by $F26P_2$. $V/K_{F6P}$, however, decreases by about 15-fold in the presence of $F26P_2$ at all pH values. An enzyme group (pK 7.4) must be unprotonated to bind $F26P_2$. It was further suggested by Payne *et al.* (1995) that $F26P_2$ activates PFK by lowering the off-rate for F6P (and probably FBP) from the binary and ternary complexes.

*Kinetic Mechanism of Ascaris suum PFK.* There has been much debate on the activation of glycogenolysis and glycolysis indicates a hormone-sensitive phosphorylation in response to the metabolic needs of the parasite. The apparent regulation by phosphorylation of the *Ascaris* PFK is different from that of rabbit muscle PFK, which is also capable of being phosphorylated *in vivo*. Phosphorylation of the rabbit muscle enzyme has been shown to be unimportant since no significant change in the kinetic or regulatory behavior has been detected (Foe & Kemp, 1982; Katajima *et al.*, 1983). All of the above findings have led researchers to suggest a coordinated regulation of glycogenolysis and glycolysis in *A. suum* involving phosphorylation.

*Desensitized Ascaris suum Phosphofructokinase.* An important step in studying the kinetic and chemical mechanism of phosphofructokinase has been the preparation of a 'desensitized' but active form of *A. suum* PFK (dPFK) which does not exhibit hysteresis, ATP inhibition, or F6P cooperativity, all of which have complicated initial velocity studies in the past (Rao *et al.*, 1987a). The dPFK is prepared by chemical modification of the native enzyme with diethylpyrocarbonate. The reaction is carried out in the presence of saturating F6P, which protects an active site histidine but allows the derivatization of an allosteric site histidine. The derivatization locks the enzyme into an active conformation which has been shown by circular dichroism to be similar to the pH-activated form of native PFK at pH 8.0 (Rao *et al.*, 1995). Both nPFK at pH 8.0 and dPFK at neutral pH are partially activated in a manner distinct from the activating effects of $F26P_2$ and AMP (Payne *et al.*, 1991). Thus, the above findings support a theory that the protonation state of a single allosteric site histidine with a pK of 6.4-6.8 determines in part the allosteric behavior of phosphofructokinase (Frieden *et al.*, 1976; Cook *et al.*, 1987; Rao *et al.*, 1987a).

Availability of a desensitized PFK has provided a means of studying the catalytic properties of the enzyme at physiological pH without the interference of the many allosteric effects that occur with the native enzyme. In contrast to the activated

conformer, dPFK, a chemically-derived less active conformer, oPFK, has also been generated using periodate-oxidized ATP (oATP; Rao *et al.*, 1991b). The authors showed that the ATP analog, oATP, modifies the native enzyme at a ratio of 2 mol/subunit, giving an enzyme form which has only 10% of the native enzyme activity. Modification by oATP was further shown to result from the modification of an allosteric site lysine (pK 8.4) while the catalytic site remains intact. Thus, the activated dPFK is prepared in the presence of saturating F6P, and the less active oPFK is prepared in the presence of a saturating amount of an ATP analog, supporting a theory that F6P stabilizes a more active conformation and ATP stabilizes a less active conformation (Cook *et al.*, 1987).

*Chemical Mechanism of Ascaris suum PFK.* The effects of pH on the dPFK-catalyzed reaction and on the $F26P_2$ activation of the enzyme have recently been studied (Payne *et al.*, 1995). pH studies are not easily carried out and interpreted with native PFK because of the many pH-dependent allosteric changes that occur. Data obtained by Payne *et al.* (1995) allowed the authors to propose an acid/base mechanism for the *A. suum* PFK (Mechanism I). Briefly, an enzyme general base (pK 7.0) accepts a proton from the 1-hydroxyl of F6P concomitant with attack on the $\gamma$-phosphate of MgATP. A second enzyme group with a pK of 8.9 must be protonated and has been proposed to be involved in neutralizing the negative charge on MgATP to facilitate the nucleophilic attack by F6P. The authors further showed that V and $V/K_{MgATP}$ are pH-independent and are not affected by $F26P_2$. $V/K_{F6P}$, however, decreases by about 15-fold in the presence of $F26P_2$ at all pH values. An enzyme group (pK 7.4) must be unprotonated to bind $F26P_2$. It was further suggested by Payne *et al.* (1995) that $F26P_2$ activates PFK by lowering the off-rate for F6P (and probably FBP) from the binary and ternary complexes.

*Kinetic Mechanism of Ascaris suum PFK.* There has been much debate on the

## MECHANISM I.

Acid-Base Mechanism for *Ascaris* PFK.

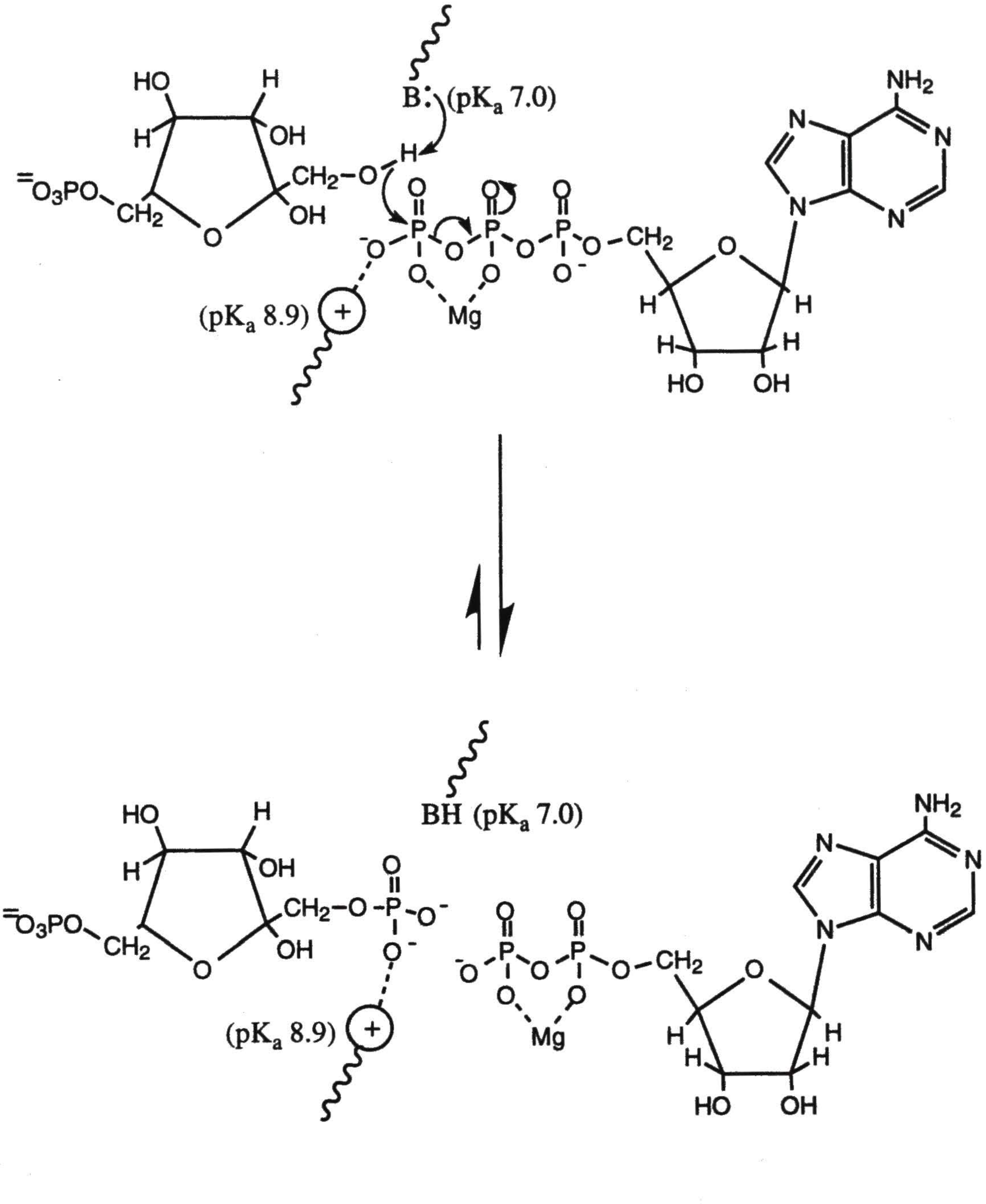
B:
(pKa 7.0)
(pKa 8.9)
Mg
BH (pKa 7.0)
(pKa 8.9)
Mg

kinetic mechanism of phosphofructokinase. The rabbit muscle enzyme is by far the best studied PFK at this time, with most of the evidence indicating a random kinetic mechanism. It was proposed by Uyeda (1970) that rabbit muscle PFK exhibited ping pong kinetics, based on parallel initial velocity patterns and the existence of both ATPase and FBPase activities. However, no phosphorylated enzyme intermediate could be isolated, and Uyeda suggested that the parallel or near-parallel initial velocity pattern could be caused by a very low $K_D/K_m$ ratio and that the mechanism may be sequential. Both Kee and Griffin (1972) and Hanson *et al.* (1973) later proposed a rapid equilibrium random mechanism for the enzyme based on initial velocity studies and equilibrium isotope exchange. Bar-Tana and Cleland (1974) also proposed a random mechanism, but suggested a steady-state rather than rapid equilibrium mechanism because of the curvature of the reciprocal plots at high substrate concentrations. Martensen and Mansour (1976) proposed ordered binding with MgATP binding before the alternative substrate fructose 6-sulfate, thus selecting one of the two pathways in the random mechanism as a result of the poor binding of fructose 6-sulfate. More recently, Merry and Britton (1985) used both flux and isotope partitioning studies to propose a random mechanism for rabbit muscle PFK with 72% of the reaction proceeding with MgATP binding before F6P. Both Bar-Tana and Cleland (1974) and Merry and Britton (1985) also noted synergistic binding of substrates with the rabbit muscle enzyme.

For all of the above-mentioned studies on the rabbit muscle PFK, experiments were carried out at pH 8.0 to avoid allosteric behavior. As mentioned, the DEPC-modified *A. suum* PFK (dPFK) has allowed kinetic studies to be carried out at neutral pH. Rao *et al.* (1987b) proposed a predominantly ordered mechanism for dPFK at pH 6.8, and also for native PFK at pH 8.0, where MgATP binds to enzyme before F6P and FBP is released from enzyme before MgADP. A minor alternative pathway in which F6P

binds to enzyme prior to MgATP was also suggested based on protection by F6P of the active site from diethylpyrocarbonate modification. However, the dissociation constant for the E:F6P complex was estimated to be 50-60 mM (Rao *et al.*, 1987a), which effectively eliminates the pathway in which F6P binds prior to MgATP at physiological levels of F6P. The ordered mechanism for *A. suum* PFK is unique for a phosphofructokinase. In addition to rabbit muscle PFK, *Escherichia coli* PFK has also been shown to have a random kinetic mechanism (Deville-Bonne *et al.*, 1991). The pyrophosphate-dependent enzyme ($PP_i$-PFK) from *Propionibacterium freudenreichii* (Cho *et al.*, 1988), *Entamoeba histolytica* (Bertagnolli & Cook, 1984), and *Phaseoleus aureus* (Bertagnolli *et al.*, 1986) all exhibit a rapid equilibrium random kinetic mechanism. The only case in which an ordered mechanism is observed is for the non-allosteric PFK from *Lactobacillus plantarum*, but the order is opposite that of the *A. suum* enzyme, with F6P binding to enzyme before MgATP (Simon & Hofer, 1978).

*Isotope Partitioning.* In order to confirm the ordered kinetic mechanism for the *A. suum* PFK and also to determine the rates of some of the steps in this reaction, experiments using the technique of isotope partitioning (Rose, 1980) have been carried out in conjunction with initial velocity studies, and the results are described in this dissertation. Isotope partitioning has been used in many multi-reactant enzyme systems to detect the presence of putative covalent intermediates or noncovalent enzyme/substrate complexes that are tightly bound (Krishnaswamy *et al.*, 1962; Rose, *et al.*, 1974; Raushel & Cleland, 1977; Landsperger *et al.*, 1978; Dann & Britton, 1978). The pulse/chase technique utilizes isotopic dilution to distinguish between the steady state turnover of an enzyme catalyzed reaction and the pre-steady state existence of a putative enzyme/substrate complex. For a ping pong mechanism where a fragment of substrate A is transferred to substrate B via a covalent enzyme intermediate F to give product Q, the isotope partitioning experiment is straightforward (Diagram I). Radiolabeled substrate A

# DIAGRAM I.

## A Typical Isotope Partitioning Experiment.

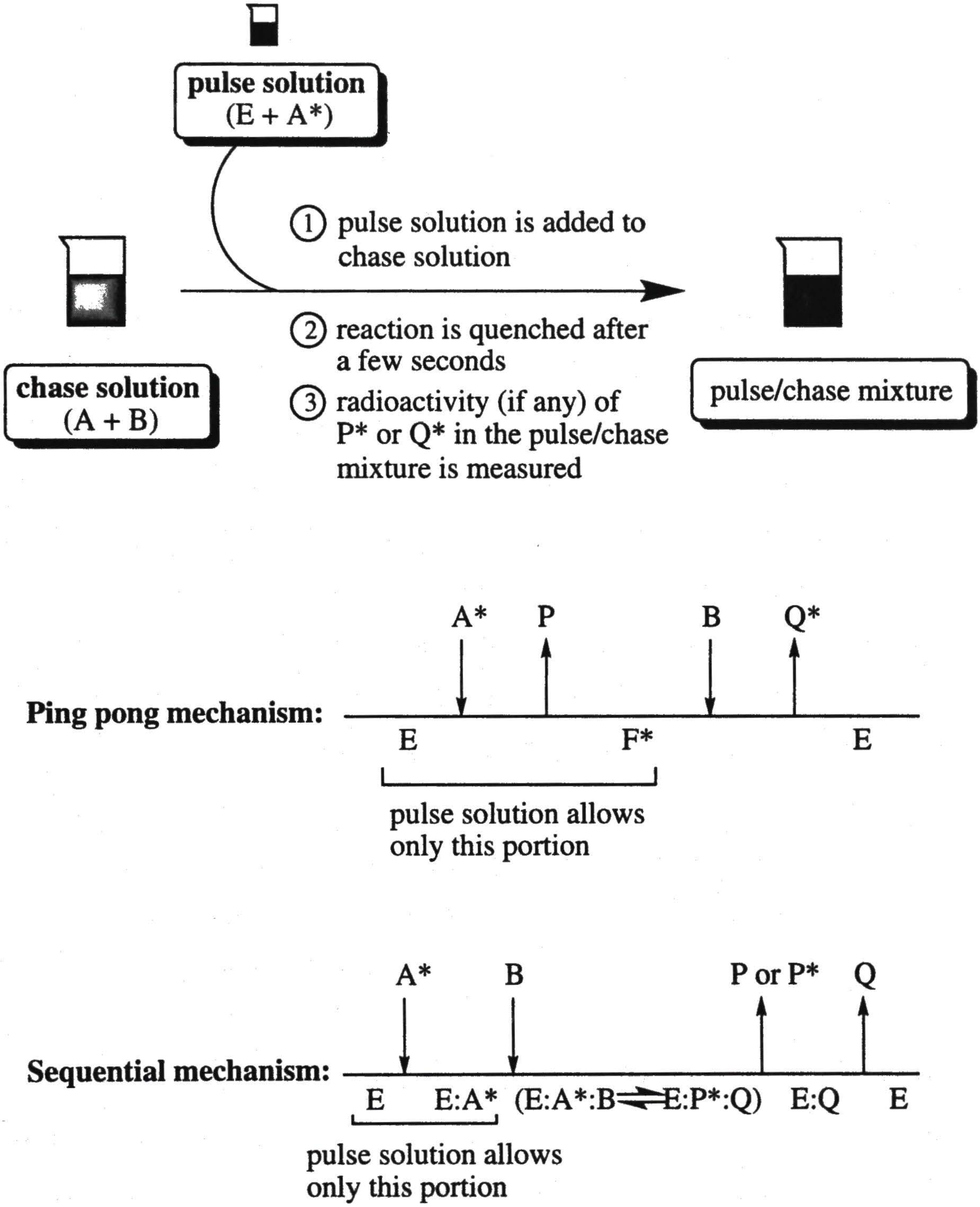
pulse solution
(E + A*)
① pulse solution is added to chase solution
chase solution
(A + B)
② reaction is quenched after a few seconds
③ radioactivity (if any) of P* or Q* in the pulse/chase mixture is measured
pulse/chase mixture
A*
P
B
Q*
Ping pong mechanism:
E
F*
E
pulse solution allows only this portion
A*
B
P or P*
Q
Sequential mechanism:
E
E:A*
(E:A*:B⇌E:P*:Q)
E:Q
E
pulse solution allows only this portion

(designated A*) is first mixed with enzyme in the absence of substrate B so that the first half-reaction (the formation of F*) is allowed, but the second half-reaction (formation of Q*) is not allowed. The 'pulse' solution (E plus A*) is then added to a 'chase' solution containing a large excess of non-radiolabeled substrate A plus substrate B, so that the second half-reaction can be completed. The large amount of non-radiolabeled A in the chase solution serves to decrease the specific radioactivity of any free A* that exists in the pulse/chase mixture. Isotopic dilution is such that any radiolabeled product Q* that is formed in the pulse/chase mixture is only from the radiolabeled covalent enzyme intermediate that was initially present in the pulse solution, and not from the steady-state turnover of enzyme in the pulse/chase mixture. Also, the pulse/chase mixture is quickly quenched so that only the first few turnovers of enzyme are measured, and not the steady-state turnover. Therefore, an enzyme exhibiting ping pong kinetics can give a positive result for this test for a covalent intermediate. That is, formation of radiolabeled product can occur,indicating that the first half-reaction can occur in the absence of the second substrate. A negative result for an enzyme where a covalent intermediate is expected would indicate that the first half-reaction is not possible in the absence of the second substrate due to structural and/or chemical constraints. Since it is probable that a covalent enzyme intermediate will survive the isotopic dilution in the pulse/chase mixture before the reaction-completing substrate binds, the extent of 'trapping' of the radiolabeled substrate for a ping pong mechanism will be independent of the concentration of chasing substrate B.

A positive result for such an isotope partitioning experiment can also be obtained for an enzyme exhibiting a sequential mechanism where no covalent intermediate occurs, provided that the noncovalent enzyme/substrate complex is converted to product in the pulse/chase mixture faster than it dissociates (Diagram I). The extent of trapping of this

substrate as product will be dependent on the concentration of the chasing substrate B. Dependence on the concentration of the second substrate distinguishes the sequential mechanism from a ping pong mechanism. If substrate trapping does occur in the sequential case, then a thorough kinetic analysis (Cleland, 1975; Rose, 1980) allows the estimation of the off-rate of substrate A from both the binary (E:A) and ternary (E:A:B) complexes. In addition to the quantitative data obtained from these experiments, other qualitative data are forthcoming. Trapping of any substrate A* as product means that the conversion of E:A* to product is fast compared to its dissociation, indicating a steady state mechanism as opposed to a rapid equilibrium mechanism. Trapping of substrate A* also indicates that A is able to bind to the enzyme in the absence of substrate B. For a random sequential mechanism, trapping of both the E:A* and the E:B* complex would be possible, while a strictly ordered mechanism where A binds before B will give no trapping of substrate B. Furthermore, if the concentration of the initial E:A* complex is known accurately, then isotope trapping provides information as to the viability of such a complex. For instance, a traditional steady state kinetic study does not account for any improperly bound substrate that may be present. On the other hand, an equilibrium binding study accounts for all substrate binding but does not reveal the functionality of this binding. Thus, the trapping of a substrate as product provides a link between the equilibrium binding of the substrate to enzyme in the pulse solution and the kinetic functionality of the complex in the chase solution.

The usefulness of an isotope partitioning study can be extended even further for an allosteric enzyme such as PFK, where partitioning parameters may change in the presence of allosteric effectors. The experiments detailed in this dissertation involve the analysis of isotope partitioning and initial velocity studies for *A. suum* native PFK (nPFK) at pH 8.0 and dPFK at pH 6.8. The effects of $F26P_2$ on the isotope partitioning and initial velocity parameters are also presented. The experiments in Chapter III were

carried out at 8 mM total $Mg^{2+}$ to ensure that all ATP in a given reaction mixture would exist as the MgATP metal-chelate complex. However, during the course of the studies presented in Chapter III, it was noticed in this laboratory that free $Mg^{2+}$ activates *A. suum* PFK, which lead to the experiments at varied $Mg^{2+}$ described in Chapter IV.

Since Rao *et al.* (1987b) reported that *A. suum* PFK exhibits a steady state ordered kinetic mechanism with MgATP binding before F6P, the first hypothesis of the research presented in this dissertation was that an isotope partitioning experiment with MgATP* as the pulse substrate will allow the formation of radiolabeled product, while an experiment with $[^{14}C]$F6P as the pulse substrate will not allow the formation of radiolabeled product. Even partial trapping of the substrate MgATP will provide an estimation of the off-rate of this substrate from the enzyme. The second hypothesis for this work was that the divalent cation $Mg^{2+}$ acts as an essential activator of *A. suum* PFK. An estimation of $K_{act}$ for $Mg^{2+}$, the equilibrium constant describing the concentration of $Mg^{2+}$ necessary to activate the enzyme to 50% of its maximal activity, will provide the groundwork for future studies on the $Mg^{2+}$ activation of *A. suum* PFK. The data for the isotope partitioning and initial velocity studies at high magnesium have been published (Gibson *et al.*, 1996), and the data for the studies with varying magnesium levels are in preparation.

# CHAPTER II

# METHODS

*Chemicals.* ($\gamma$-$^{32}$P)ATP and (U-$^{14}$C)FBP were purchased from ICN Radiochemicals. (U-$^{14}$C)F6P was prepared from (U-$^{14}$C)FBP in a 0.5 mL reaction mixture containing 50 mM Tris-HCl, pH 7.5, 5 mM $MgCl_2$, 0.1 mM EDTA, 0.1 unit of D-fructose 1,6-bisphosphatase, and 5 μCi of (U-$^{14}$C)FBP. After 30 minutes, greater than 95% of the radioactivity copurified with (U-$^{14}$C)F6P on anion exchange chromatography. The reaction mixture was passed through a Centricon-100 membrane to remove the bisphosphatase and was used without further purification. All other chemicals and enzymes were purchased from Sigma.

*Purification of Ascaris suum PFK.* Phosphofructokinase from *Ascaris suum* was purified according to the method of Starling *et al.* (1982) with the exception of the addition of the protease inhibitors aprotinin (10 mg/L), trypsin inhibitor (20 mg/L), and phenylmethylsulfonyl fluoride (1 mM) to the crude extract and the DEAE-Sephacel eluate. The purified enzyme had a final specific activity of approximately 43 units/mg. The enzyme was stored in 50 mM $KH_2PO_4$ buffer, pH 7.5, with 2% glycerol and 10 mM BME. For initial velocity experiments, the enzyme was diluted with the same storage buffer to approximately 5 units/mL. For isotope partitioning experiments, the enzyme was concentrated to approximately 500 units/mL using an Amicon conical membrane centrifuge apparatus with a molecular weight cutoff of 30,000 Da.

*Chemical Modification of native PFK.* The dPFK was prepared according to the method of Rao *et al.* (1987a), giving a final specific activity of 30 units/mg. The dPFK

was stored in 50 mM $KH_2PO_4$ buffer, pH 6.8, with 2% glycerol and 10 mM BME. The concentration of the dPFK in initial velocity and isotope partitioning experiments was the same as for the native enzyme. The protein concentration of both nPFK and dPFK was determined by the method of Bradford (1976) with bovine serum albumin as a standard.

*Initial Velocity Studies.* All assays in the direction of phosphorylation of F6P were obtained by coupling product formation to the disappearance of NADH and monitoring the absorbance at 340 nm. The formation of FBP was coupled to the aldolase/triosephosphate isomerase/α-glycerol phosphate dehydrogenase reactions where a typical 1 mL reaction mixture contained 100 mM imidazole-HCl, pH 6.8 (or 100 mM Tris-HCl, pH 8.0), 8 mM $MgCl_2$, 14 units of aldolase, 34 units of triosephosphate isomerase, 4 units of α-glycerolphosphate dehydrogenase, 0.2 mM NADH, ATP and F6P in the amounts indicated, and 20 milliunits of PFK. MgADP formation was coupled to the pyruvate kinase/lactate dehydrogenase reactions where a typical 1 mL reaction mixture contained 100 mM imidazole-HCl, pH 6.8 (or 100 mM Tris-HCl, pH 8.0), 8 mM $MgCl_2$, 3 units of pyruvate kinase, 3 units of lactate dehydrogenase, 100 mM KCl, 0.2 mM NADH, 0.2 mM PEP, ATP and F6P in the amounts indicated, and 20 milliunits of PFK. In the initial velocity and inhibition experiments, a double coupled assay was used which monitors the production of both FBP and MgADP in the same 1 mL cuvette. This double coupled assay gives greater sensitivity than either assay alone, avoids product inhibition by removing both products, and gives longer linear time courses by recycling ATP. All assays were initiated with PFK.

Initial velocity patterns were determined using the double coupled assay by varying MgATP at several fixed concentrations of F6P. Inhibition patterns were also determined using the double coupled assay by fixing F6P equal to its $K_m$ value and varying MgATP at several different concentrations of inhibitor. The individual $K_m$ and V values which are used in the isotope partitioning calculations were determined using the

aldolase/triose phosphate isomerase/α-glycerolphosphate dehydrogenase coupled assay by fixing one substrate at a saturating concentration and varying the other substrate. To avoid activation of PFK by $(NH_4)_2SO_4$, all coupling enzyme stock solutions were made either by desalting an ammonium sulfate suspension of the enzyme using a Centricon-30 centrifuge/filter apparatus or by dissolving a lyophilized powder of the enzyme.

*$Mg^{2+}$ Chelate Correction.* All previous *A. suum* PFK initial velocity experiments as well as the first isotope partitioning experiments in this dissertation were carried out at an arbitrarily high $[Mg^{2+}]$ concentration so that all ATP would be present as MgATP, the true substrate for PFK. However, in studying the effect of the $Mg^{2+}$ ion on this enzyme it has become necessary to fix the $Mg^{2+}$ concentration to an exact value by correcting for all Mg-ligand complexes present in a reaction mixture. The concentration of substrates, effectors, and inhibitors were corrected for the concentration of any metal-ligand complex at a given $[Mg^{2+}]_{free}$ concentration using eq 1:

$$[L]_t = [L]_{free} + \frac{[L]_{free}[Mg^{2+}]_{free}}{K_{ML}} \qquad (1)$$

where $[L]_t$ is the total concentration of ligand in the reaction mixture, $[L]_{free}$ is the desired concentration of free ligand, $[Mg^{2+}]_{free}$ is the desired concentration of free $Mg^{2+}$, and $K_{ML}$ is the equilibrium constant for dissociation of the Mg-ligand complex. The total concentration of $Mg^{2+}$ ions to be added to a reaction mixture containing *i* ligands was calculated according to eq 2:

$$[Mg^{2+}]_t = [Mg^{2+}]_{free} + \Sigma\frac{[Mg^{2+}]_{free}[L_i]_{free}}{K_{MLi}} \qquad (2)$$

where $[Mg^{2+}]_t$ is the total concentration of $Mg^{2+}$ to be added to the reaction mixture,

$[L_i]_{free}$ is the desired concentration of the *i*th ligand, and $K_{ML_i}$ is the equilibrium constant for dissociation of the chelate complex between $Mg^{2+}$ and the *i*th ligand. For the purposes of this dissertation, results at 'low' $Mg^{2+}$ are those obtained at the fixed $Mg^{2+}$ concentration of 0.1 mM, while experiments at 'high' $Mg^{2+}$ are those obtained at 2 mM or higher $Mg^{2+}$ concentration.

The dissociation constant for the MgATP complex was taken from Dawson *et al.* (1986) as 15 µM, while the dissociation constant for the MgF6P complex was taken from Martell & Smith (1982) as 25 mM. The dissociation constant for the $MgF26P_2$ complex has not been reported, but is assumed to be similar to that of Mg-glucose 1,6-bisphosphate, taken from Dawson *et al.* (1986) as 7 mM. The dissociation constant for the MgAra5P complex also has not been reported, but is assumed to be similar to that of MgF6P.

*Circular Dichroism Spectral Measurements.* Circular dichroic spectra were recorded using an Aviv model 62 DS CD spectrometer maintained at a constant temperature of 10°C. Samples contained 0.2 mg/mL enzyme in 20 mM $KH_2PO_4$ plus 8 mM $MgCl_2$, at either pH 6.8 (for dPFK) or pH 8.0 (for nPFK), in 0.2-cm quartz cuvettes. Spectra were recorded from 250 to 200 nm at intervals of 1 nm and a dwell time of 3 s. Each spectrum was the average of two repetitions, and buffer blanks were substracted from each spectrum. Titrations were carried out in a single cuvette by adding 2-µL increments of stock ATP so that final MgATP concentrations ranged from 0.4 to 10.1 µM and the total volume increased by less than three percent. The increase in ellipticity at 222 nm for each concentration of MgATP was then fitted using eq 3 to obtain the calculated dissociation constant for the E:MgATP complex.

*Isotope Partitioning Studies.* Isotope partitioning experiments were performed at 30°C according to the method of Rose (1980) at 8 mM $Mg^{2+}$ for the dPFK:MgATP*,

nPFK:MgATP*, and dPFK:[U-$^{14}$C]F6P complexes, and at 0.1 mM $Mg^{2+}$ for the dPFK:MgATP* complex. These experiments were carried out both in the absence and in the presence of $F26P_2$. The methods for the experiments at high $Mg^{2+}$ are described first, followed by the methods for the experiments at low $Mg^{2+}$.

For the high $Mg^{2+}$ dPFK:MgATP* experiment in the absence of $F26P_2$, the pulse consisted of 130 µM dPFK (based on MW = 90,000 per subunit) and 0.24 mM MgATP* (9,000 cpm/nmol) in a total volume of 50 µL. The chase consisted of 100 mM imidazole-HCl (pH 6.8), 2.0 mM MgATP, and 0.5, 1.0, 4.2, or 10.0 mM F6P in a total volume of 5 mL. Using a $K_D$ value of 2.0 µM for the dPFK:MgATP* complex at 8 mM $Mg^{2+}$, $[\text{dPFK:MgATP*}]_0$ is 129 µM. For experiments in the presence of saturating $F26P_2$, the pulse consisted of 60 µM dPFK, 0.24 mM MgATP* (9,000 cpm/nmol), and 0.2 mM $F26P_2$ in a total volume of 50 µL, and the chase consisted of 100 mM imidazole-HCl (pH 6.8), 2.0 mM MgATP, and 0.2, 0.5, 1.0, or 10.0 mM F6P plus 0.2 mM $F26P_2$ in a total volume of 5 mL. Using a $K_D$ value of 2.3 µM for the dPFK:MgATP* complex at 8 mM $Mg^{2+}$, $[\text{dPFK:MgATP*}]_0$ is 59 µM.

For the high $Mg^{2+}$ nPFK:MgATP* experiments in the absence or presence of saturating $F26P_2$, the pulse consisted of 55 µM nPFK, 0.2 mM MgATP* (10,000 cpm/nmol), plus and minus 0.2 mM $F26P_2$ in a total volume of 50 µL, and the chase consisted of 100 mM Tris-HCl (pH 8.0), 2.0 mM MgATP, and 0.1, 0.2, 2.0, or 10.0 mM F6P, plus and minus 0.2 mM $F26P_2$ in a total volume of 5 mL. Using a $K_D$ of 2.0 µM for the nPFK:MgATP* complex at 8 mM $Mg^{2+}$ in the absence of $F26P_2$, $[\text{nPFK:MgATP*}]_0$ is 54 µM. Using a $K_D$ of 5.7 µM for the nPFK:MgATP* complex in the presence of $F26P_2$, $[\text{nPFK:MgATP*}]_0$ is 53 µM.

For the high $Mg^{2+}$ dPFK:[U-$^{14}$C]F6P experiments in the presence of saturating $F26P_2$, the pulse consisted of 90 µM dPFK, 1 mM [U-$^{14}$C]F6P (2,000 cpm/nmol), and 0.2 mM $F26P_2$ in a total volume of 50 µL, and the chase consisted of 100 mM imidazole

(pH 6.8), 1 mM MgATP, 10 mM F6P, and 0.2 mM $F26P_2$ in a total volume of 5 mL. The $K_D$ for the E:F6P complex at high $Mg^{2+}$ in the absence of $F26P_2$ has been estimated to be 50 to 60 mM (Rao *et al.*, 1987a). $F26P_2$ has been shown to decrease $K_{F6P}$ by 15-fold (Payne *et al.*, 1991), presumably by decreasing the off-rate for F6P. Whether the off-rate is decreased or the rate of the turnover of the central complexes is increased, trapping of an E:[U-$^{14}$C]F6P complex is more likely to occur in the presence of $F26P_2$ than in the absence of this effector. It can be assumed that if no significant trapping occurs in the presence of $F26P_2$, then no trapping should occur in the absence of $F26P_2$ since either the initial binary complex is more difficult to form or the turnover of central complexes is slower. It is not feasible to study $^{14}$C-F6P trapping in the absence of $F26P_2$ due to the high concentrations of $^{14}$C-F6P necessary to form the initial E:$^{14}$C-F6P complex in the pulse solution and the large dilution of unlabeled F6P that is necessary in the chase solution.

For the low $Mg^{2+}$ dPFK:MgATP* experiments in the absence or presence of $F26P_2$, the pulse consisted of 0.1 mM dPFK, 0.2 mM MgATP* (10,000 cpm/nmol), plus and minus 0.2 mM $F26P_2$ in a total volume of 50 µL. The chase consisted of 50 mM imidazole-HCl (pH 6.8), 2.0 mM MgATP, and 0.25, 0.5, 10.0, or 20.0 mM F6P in a total volume of 5 mL. Using a $K_D$ value of 30 µM for the dPFK:MgATP complex at 0.1 mM $Mg^{2+}$ in the absence of $F26P_2$, $[\text{dPFK:MgATP}]_0$ is 80 µM. Using a $K_D$ value of 38 µM in the presence of $F26P_2$, $[\text{dPFK:MgATP}]_0$ is 76 µM.

In order to allow a reliable comparison of the isotope partitioning data at 0.1 mM $Mg^{2+}$ to the data at high $Mg^{2+}$, experiments at high $Mg^{2+}$ were repeated using the same enzyme stock as that used in the low $Mg^{2+}$ experiments. The $Mg^{2+}$ concentration was fixed at 5 mM, correcting for the formation of MgATP and MgF6P as was done in all experiments at low and varied $Mg^{2+}$. The pulse consisted of 0.1 mM dPFK, 0.2 mM MgATP* (10,000 cpm/nmol), plus and minus 0.2 mM $F26P_2$ in a total volume of 50 µL.

The chase consisted of 50 mM imidazole-HCl (pH 6.8), 2.0 mM MgATP, and 0.5 or 10.0 mM F6P in a total volume of 5 mL. Assuming a $K_D$ value of 2 µM for the dPFK:MgATP complex at high $Mg^{2+}$, $[dPFK:MgATP]_0$ is 98 µM.

For all isotope partitioning experiments, the pulse was added to the rapidly stirring chase solution, and the reaction was quenched after 3 seconds by adding 200 µmoles of EDTA. A 1 mL aliquot of the quenched reaction mix was then injected onto a Whatman Partisil 10-SAX column with 250 mM phosphate as the running buffer, a gradient from 0-1.5 M KCl, and a flow rate of 2 mL/min. Fractions of 2 mL were collected and the amounts of MgATP*/[1-$^{32}$P]FBP and [U-$^{14}$C]F6P/[U-$^{14}$C]FBP were determined by scintillation counting. For each experiment two controls were done. Control 1 was a zero-point for the substrate varied in the chase, thus accounting for any ATPase reaction in the pulse solution. This control was necessary because $P_i$ and FBP coelute from the anion exchange column under these conditions. Control 2 was carried out for each concentration of varied chase substrate by placing the radiolabeled substrate only in the chase solution, thus accounting for any steady-state production of radiolabeled product in the pulse/chase mixture. All data points and controls were the average of duplicate experiments.

*Data Analysis*. Steady-state kinetic data were fitted using the appropriate rate equations and computer programs developed by Cleland (1979). Equation 3 was used for substrate saturation curves. Equation 4 was used for initial velocity patterns in the absence of inhibitors. Equations 5 and 6 were used for uncompetitive, and noncompetitive inhibition patterns, respectively, where one substrate was fixed and the other substrate was varied at several different concentrations of inhibitor. Equation 7 was used for the initial velocity pattern at varied $Mg^{2+}$ and MgATP with F6P fixed. Partitioning data were fitted using equation 3 with $P^*$ and $P^*_{max}$ substituted for v and V, and $K'_a$ ($K_m$ for trapping) substituted for $K_a$.

$$v = \frac{VA}{K_a + A} \tag{3}$$

$$v = \frac{VAB}{K_{ia}K_b + K_aB + K_bA + AB} \tag{4}$$

$$v = \frac{VA}{K_a + A(1 + \frac{I}{K_{is}})} \tag{5}$$

$$v = \frac{VA}{K_a\,(1 + \frac{I}{K_{is}}) + A\,(1 + \frac{I}{K_{ii}})} \tag{6}$$

$$v = \frac{VAB}{K_{ia}K_b + K_bA + AB} \tag{7}$$

In eqs 3-7 v and V are initial and maximum velocities, A, B, and I are reactant and inhibitor concentrations, $K_a$ and $K_b$ are Michaelis constants for A and B, and $K_{ia}$, $K_{is}$, and $K_{ii}$ are inhibition constants for A, slope, and intercept, respectively.

# CHAPTER III

## ISOTOPE PARTITIONING AND INITIAL VELOCITY STUDIES WITH PHOSPHOFRUCTOKINASE AT HIGH $[Mg^{2+}]_{free}$

The isotope partitioning technique of Rose (1980) has been used to study the kinetic mechanism of phosphofructokinase from *Ascaris suum*. As described in Chapter I, the technique can give qualitative as well as quantitative information about a kinetic mechanism. In order to utilize the full potential of isotope partitioning, several parameters for the enzyme must be known. Most importantly, an accurate measurement of the concentration of enzyme is essential to an isotope partitioning experiment. Secondly, the dissociation constant ($K_D$) for the putative enzyme/substrate complex of interest must be known so that the initial concentration of the complex in the pulse solution can be calculated. Finally, the steady state parameters $V/E_t$ and $K_{F6P}$ must be known so that calculation of the off-rate of the substrate from the binary complex is possible. The current chapter describes first the results of the measurement of these parameters, followed by the results from the isotope partitioning experiments.

As mentioned in Chapter II, the preparations of nPFK and dPFK give specific activities of 43 U/mg and 30 U/mg, respectively. The decrease in specific activity of dPFK from the nPFK from which it is prepared is probably caused both by a loss of a number of active sites and by a slight perturbation of the tertiary structure of the enzyme, both due to chemical modification by DEPC. The dPFK concentration, however, can be assumed for these studies to have an upper limit equal to the concentration of nPFK, and a lower limit not less than 80% of the upper limit (Rao *et al.*, 1987a). The specific

activities of the nPFK and the dPFK give turnover numbers ($V/E_t$) of 65 ± 3 $s^{-1}$ and 42 ± 1 $s^{-1}$, respectively (Table 1). The $V/E_t$ values are $F26P_2$-independent, and are in excellent agreement with the data reported by Payne *et al.* (1991; 1995).

*$K_D$ Determination.* The dissociation constant ($K_D$) for an enzyme:substrate complex can generally be estimated graphically from initial velocity pattern replots and/or a computer fit of the rate equation to the data. However, a large error can be associated with such an estimate if the dissociation constant is very small ($\leq$ 1 μM) . In such cases, equilibrium binding techniques can be used to determine the $K_D$. For a substrate or effector that causes a structural change in the enzyme upon binding, the structural change can sometimes be monitored spectroscopically by a technique such as fluorescence or circular dichroism (Rao *et al.*, 1991a). A titration of the enzyme with substrate or effector while monitoring the extent of any structural change then allows an estimation of the $K_D$.

For *A. suum* phosphofructokinase, the initial velocity patterns for both nPFK and dPFK at 8 mM $Mg^{2+}$ give dissociation constants for the E:MgATP complex that are undefined due to large associated errors. The technique of circular dichroism (CD) was thus used as described in Chapter II to monitor any possible structural changes upon forming the E:MgATP complex. A structural change is in fact seen, and a typical CD spectrum of the *A. suum* PFK at zero and 10 μM of MgATP is shown in Figure 1. The reciprocal of the increase in ellipticity at 222 nm (corresponding to α-helical structure) for nPFK and dPFK in the absence or presence of $F26P_2$ versus the reciprocal of the MgATP concentration is linear (Figure 2), and a fit of eq 3 to the data gives an estimate of the dissociation constant for the E:MgATP complex. For nPFK, the $K_D$ for the E:MgATP complex is 2.0 ± 0.6 μM in the absence of $F26P_2$ and 6 ± 3 μM in the presence of $F26P_2$. For dPFK, the $K_D$ is 2.0 ± 0.5 μM in the absence of $F26P_2$ and

Table 1. Summary of Data from Isotope Partitioning of E:MgATP* with *Ascaris* PFK at High $Mg^{2+}$

| | nPFK | | dPFK | |
|---|---|---|---|---|
| | $-F26P_2$ | $+F26P_2$ | $-F26P_2$ | $+F26P_2$ |
| $V/E_t$ ($s^{-1}$) | 65 ± 3 | 65 ± 3 | 42 ± 1 | 42 ± 1 |
| $K_{F6P}$ (mM)[a] | 1.0 ± 0.1 | 0.07 ± 0.02 | 0.86 ± 0.06 | 0.10 ± 0.01 |
| $K_{iMgATP}$ (μM)[b] | 2.0 ± 0.6 | 6 ± 3 | 2.0 ± 0.5 | 2.3 ± 0.7 |
| $P^*_{max}$ (μM) | 51 ± 2 (94 ± 4%) | 48 ± 2 (89 ± 4%) | 110 ± 10 (85 ± 8%) | 32 ± 2 (54 ± 3%)[c] |
| $K'_{F6P}$ (mM) | 0.54 ± 0.09 | 0.40 ± 0.06 | 0.85 ± 0.15 | 0.26 ± 0.07 |
| $[E:A]_0/P^*_{max}$ | 1.06 ± 0.11 | 1.12 ± 0.11 | 1.18 ± 0.11 | 1.85 ± 0.11 |
| $k_{off}$ ($s^{-1}$) | 34 ± 7 | 370 ± 120 | 42 ± 8 | 110 ± 30<br>to 200 ± 45 |
| $k_7/k'_5$ | - | - | - | 0.85 ± 0.05 |
| $k_7$ ($s^{-1}$) | - | - | - | 36 ± 2 |
| $k_{on}$ ($M^{-1}s^{-1}$) | $(1.7 \pm 0.7) \times 10^7$ | $(6.2 \pm 3.2) \times 10^7$ | $(2.1 \pm 0.7) \times 10^7$ | $(4.8 \pm 2.9) \times 10^7$<br>to<br>$(8.7 \pm 3.7) \times 10^7$ |

[a] All $K_{F6P}$ values were determined using the single aldolase/triosephosphate isomerase/α-glycerolphosphate dehydrogenase coupled assay with coupling enzyme solutions made fresh from lyophilized powder to avoid the affects of $(NH_4)_2SO_4$ on $K_{F6P}$.

[b] Calculated from the CD studies.

[c] The dPFK used in the experiments for isotope partitioning in the presence of $F26P_2$ was from a separate preparation than that used for experiments in the absence of $F26P_2$. The specific activity of both preparations was 30 U/mg, but the final concentration of enzyme used in the presence of $F26P_2$ was lower than that of the enzyme used in the absence of $F26P_2$, giving a lower concentration of the initial binary complex. The 54% trapping is calculated based on the lower concentration of binary complex and is not directly comparable to the absolute trapping in the absence of $F26P_2$. As a control, the $-F26P_2$ experiment was repeated with this enzyme preparation and approximately 85% trapping was obtained. However, limited amounts of enzyme from this preparation allowed only 3 data points to be measured, so data obtained using the previous preparation (with 4 data points, Figure 5) is shown.

Figure 1. Typical circular dichroism spectra for *Ascaris suum* phosphofructokinase in the absence of MgATP (open circles) and in the presence of 10 μM MgATP (filled circles) at approximately 8 mM $Mg^{2+}$.

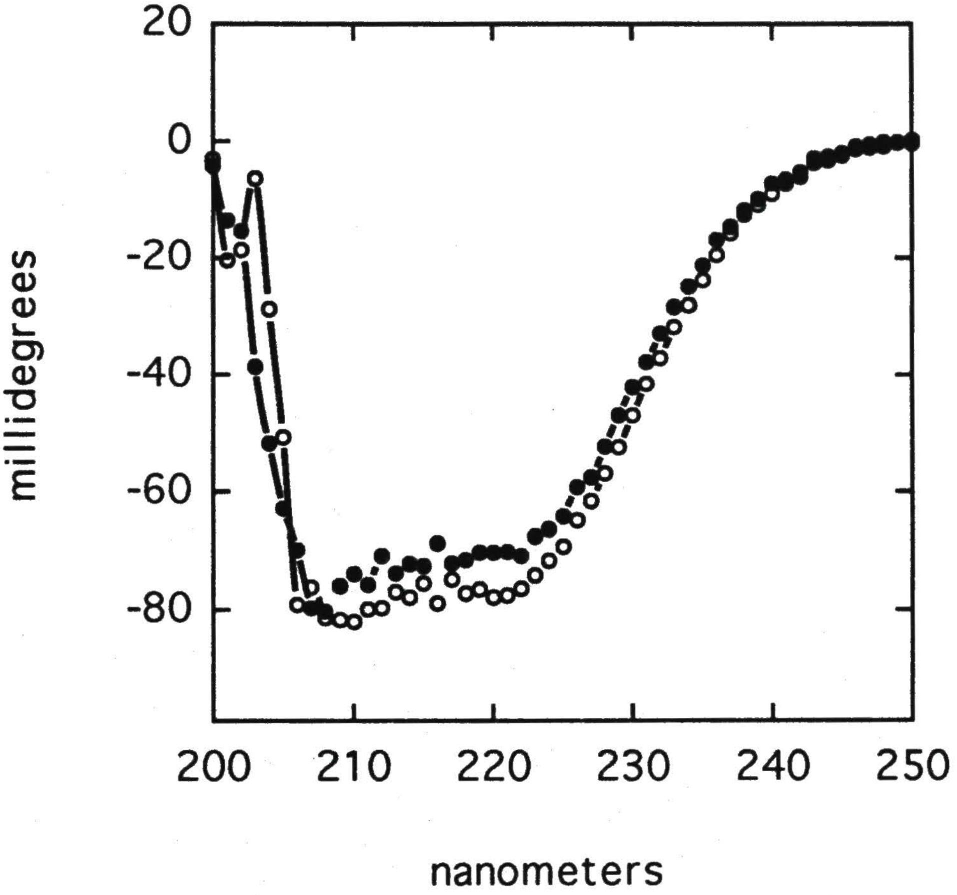
20
0
-20
-40
-60
-80
millidegrees
200
210
220
230
240
250
nanometers

Figure 2. Plot of the reciprocal change in ellipticity at 222 nanometers versus the reciprocal MgATP concentration. The data were fitted using eq 3, where v and V are substituted by $\Delta\emptyset_{222}$ and $\Delta\emptyset_{222\mathrm{max}}$, A represents the concentration of MgATP, and $K_a$ represents the dissociation constant ($K_D$) of the E:MgATP complex.

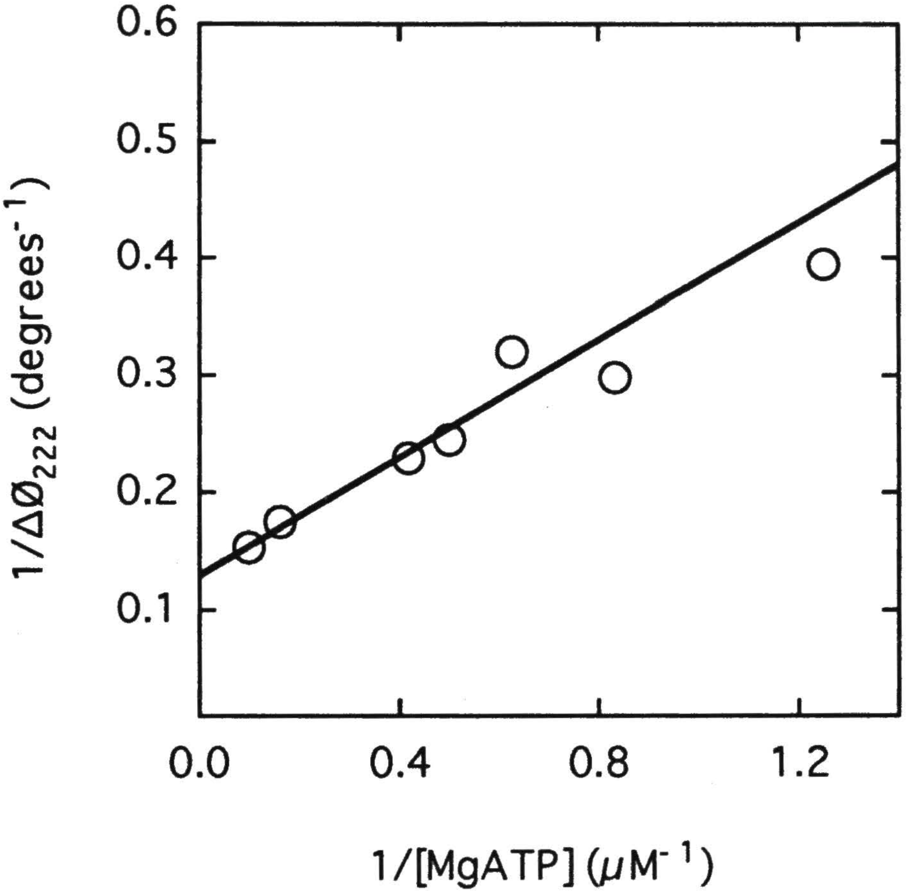
0.6
0.5
0.4
0.3
0.2
0.1
$1/\Delta\text{Ø}_{222}$ (degrees$^{-1}$)
0.0
0.4
0.8
1.2
1/[MgATP] ($\mu$M$^{-1}$)

2.3 ± 0.7 µM in the presence of $F26P_2$. The data are summarized in Table 1.

*Isotope Partitioning of nPFK:MgATP* in the Absence or Presence of* $F26P_2$. The amount of the nPFK:MgATP* trapped as a function of the F6P concentration in the chase solution is shown in Figures 3 and 4. Figure 3 shows the trapping in the absence of $F26P_2$ with a $P^*_{max}$ of 0.051 ± 0.002 mM estimated, representing 94% of the 54 µM MgATP* present in the initial binary complex ($[nPFK{:}Mg^*ATP]_0$), calculated using a $K_D$ of 2.0 µM. A $K'_{F6P}$ of 0.54 ± 0.09 mM is estimated. Figure 4 shows the partitioning data in the presence of 0.2 mM $F26P_2$, giving a $P^*_{max}$ of 0.048 ± 0.002 mM, within error equal to the $P^*_{max}$ obtained in the absence of $F26P_2$. The $K'_{F6P}$ value decreases only slightly to 0.40 ± 0.06 mM in the presence of $F26P_2$. Data are summarized in Table 1.

*Isotope Partitioning of dPFK:MgATP* in the Absence or Presence of* $F26P_2$. The amount of the dPFK:MgATP* trapped as a function of the F6P concentration in the chase solution is shown in Figures 5 and 6. Figure 5 shows that trapping in the absence of $F26P_2$ gives a $P^*_{max}$ of 0.11 ± 0.01 mM, or 85% trapping of the 129 µM MgATP* initially present in the pulse solution binary complex, estimated using a $K_D$ of 2.0 µM. The $K'_{F6P}$ for the pulse/chase reaction in the absence of $F26P_2$ is 0.85 ± 0.15 mM. Figure 6 shows the trapping of dPFK:MgATP* in the presence of 0.2 mM $F26P_2$. A $P^*_{max}$ of 0.032 ± 0.002 mM is obtained, estimated as 54% trapping of the 59 µM MgATP* initially present in the pulse solution binary complex, calculated using a $K_D$ of 2.3 µM. A $K'_{F6P}$ for trapping in the presence of $F26P_2$ of 0.26 ± 0.07 mM is obtained, a value 3.3-fold lower than the value in the absence of $F26P_2$. Data are again summarized in Table 1.

*Isotope Partitioning of dPFK:[*$^{14}$*C]F6P.* No trapping of the dPFK:[$^{14}$C]F6P complex as [$^{14}$C]FBP was detected in the presence of $F26P_2$ (see Chapter II).

Figure 3. Isotope trapping of the E:MgATP* complex with *Ascaris suum* nPFK (pH 8.0) in the absence of $F26P_2$ . The amount of [1-$^{32}$P]FBP formed at different concentrations of F6P in the chase solution was determined as described in the text. The lines are the best fit of the data using eq 3, while the points are experimental values.

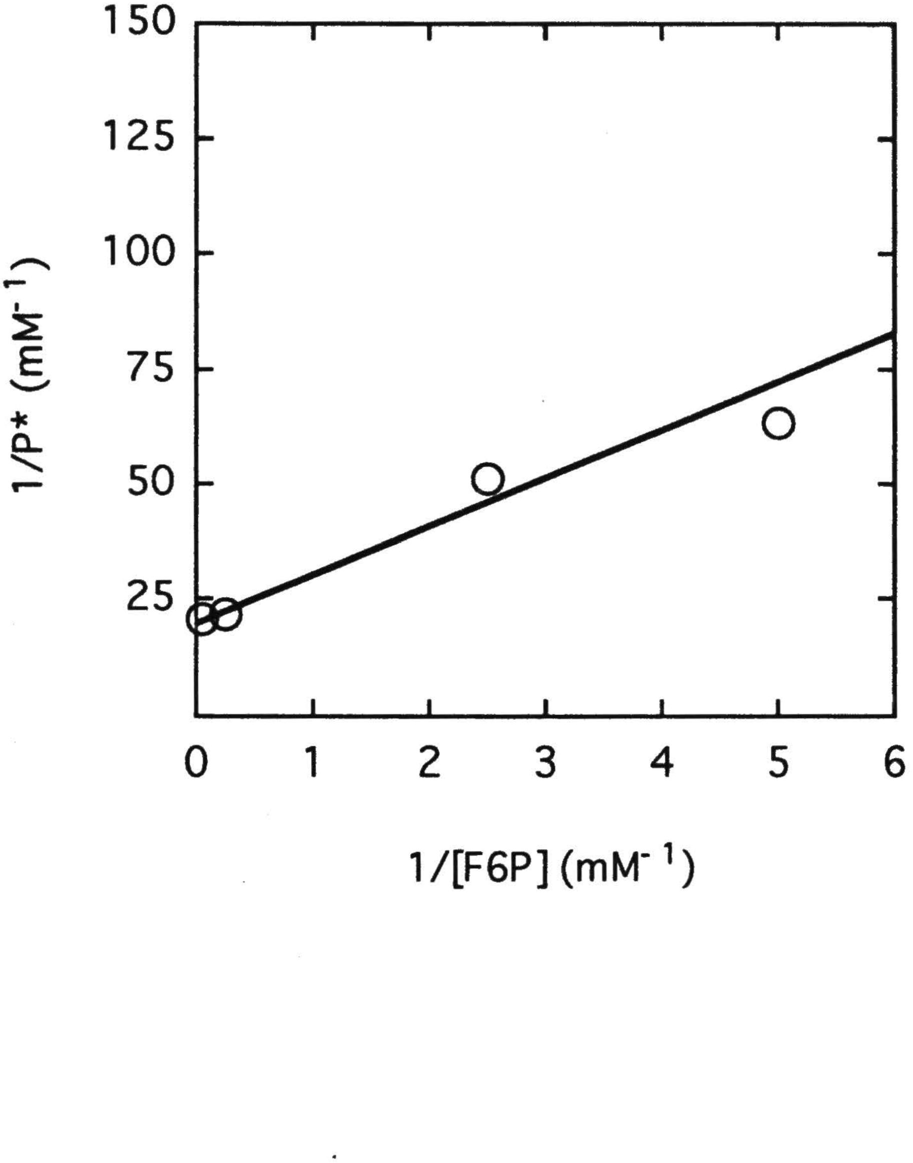
150
125
100
75
50
25
0
1
2
3
4
5
6
1/P* (mM⁻¹)
1/[F6P] (mM⁻¹)

Figure 4. Isotope trapping of the E:MgATP* complex with *Ascaris suum* nPFK (pH 8.0) in the presence of 0.2 mM F26$P_2$. The amount of [1-$^{32}$P]FBP formed at different concentrations of F6P in the chase solution was determined as described in the text. The lines are the best fit of the data using eq 3, while the points are experimental values.

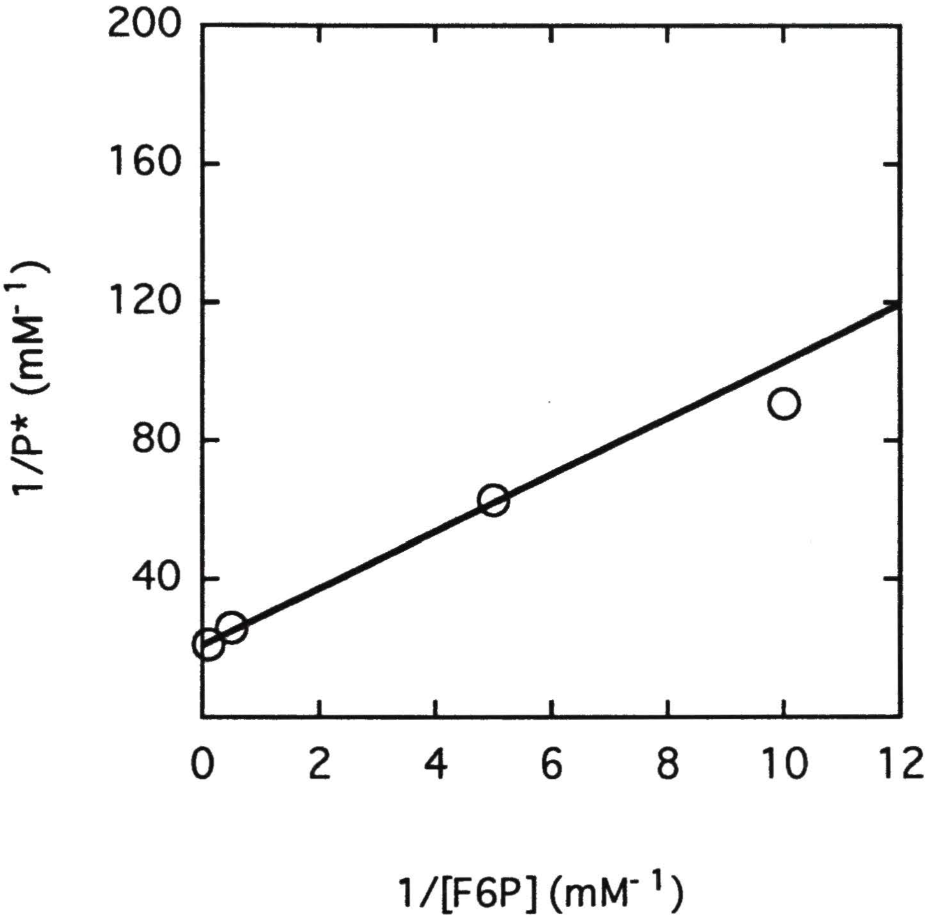
200
160
120
80
40
0
2
4
6
8
10
12
1/P* (mM⁻¹)
1/[F6P] (mM⁻¹)

Figure 5. Isotope trapping of the E:MgATP* complex with *Ascaris suum* dPFK (pH 6.8) in the absence of $F26P_2$. The amount of [1-$^{32}$P]FBP formed at different concentrations of F6P in the chase solution was determined as described in the text. The lines are the best fit of the data using eq 3, while the points are experimental values.

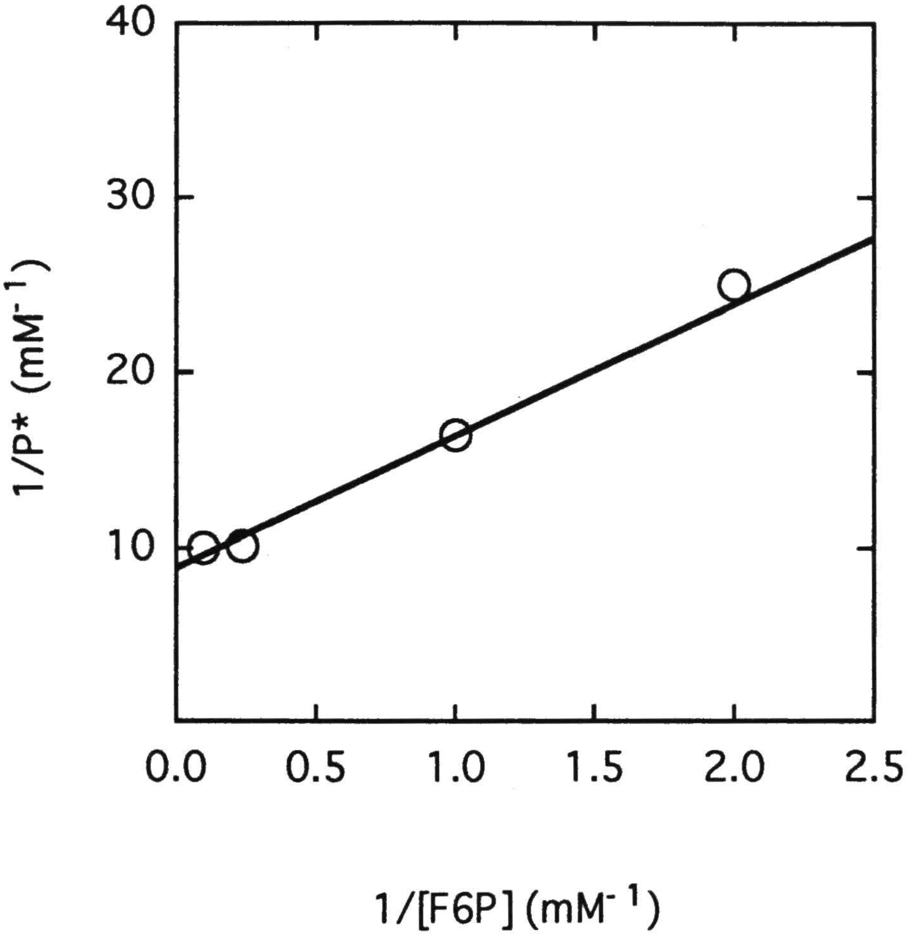
40
30
20
10
0.0
0.5
1.0
1.5
2.0
2.5
1/P* (mM$^{-1}$)
1/[F6P] (mM$^{-1}$)

Figure 6. Isotope trapping of the E:MgATP* complex with *Ascaris suum* dPFK (pH 6.8) in the presence of 0.2 mM F26$P_2$. The amount of [1-$^{32}$P]FBP formed at different concentrations of F6P in the chase solution was determined as described in the text. The lines are the best fit of the data using eq 3, while the points are experimental values.

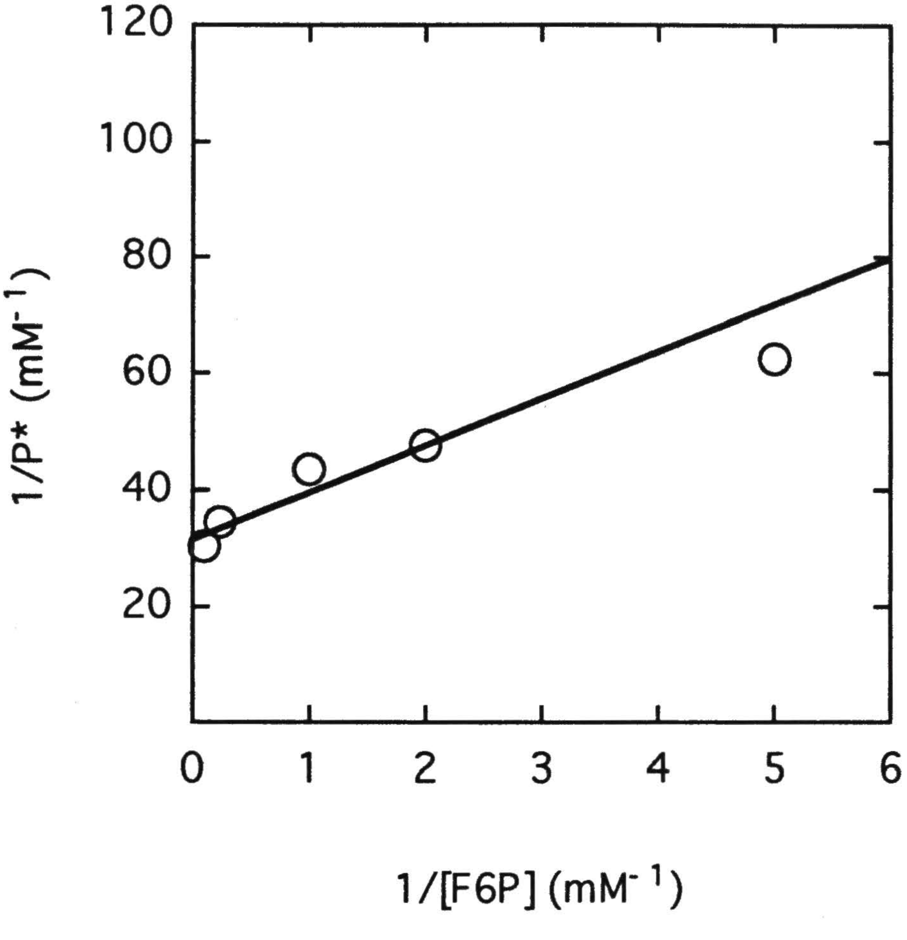
120
100
80
60
40
20
1/P* (mM$^{-1}$)
0
1
2
3
4
5
6
1/[F6P] (mM$^{-1}$)

*Initial Velocity Studies.* Initial velocity patterns in the absence or presence of 0.2 mM $F26P_2$ for both nPFK and dPFK were measured using the double coupled assay described in Chapter II, and all give similar results. A typical initial velocity pattern is shown in Figure 7. The pattern exhibits near-parallel lines suggesting a very low $K_D$ for MgATP relative to the $K_m$ for MgATP. The fit of the dPFK pattern in the presence of $F26P_2$ gives a $K_{MgATP}$ value of 17 ± 4 μM, a $K_{F6P}$ value of 72 ± 21 μM, and a $K_D$ for MgATP that is undefined.

The arabinose 5-phosphate (Ara5P) inhibition patterns in the presence of 0.2 mM $F26P_2$ were also measured using the double coupled assay and are shown in Figures 8 and 9. Data for nPFK, Figure 8, adhere to uncompetitive inhibition, while data for dPFK, Figure 9, adhere to noncompetitive inhibition. The uncompetitive inhibition pattern for nPFK yields a $K_{MgATP}$ of 7.0 ± 0.4 μM, and a $K_{ii}$ of 12.0 ± 0.5 mM for Ara5P, while the noncompetitive pattern for dPFK gives a $K_{MgATP}$ of 10 ± 1 μM, and $K_{is}$ and $K_{ii}$ values for Ara5P of 12 ± 3 mM and 10 ± 1 mM, respectively.

While the initial velocity patterns are useful in that they give estimates of the dissociation constants for both substrates, the estimated $K_m$ and V values from these patterns can have relatively large standard errors. For this reason, the $K_m$ and $V/E_t$ values used in the isotope partitioning calculations were determined from single saturation curves as described in Chapter II. The results are shown in Table 1. $V/E_t$ values are 65 ± 3 $s^{-1}$ and 42 ± 1 $s^{-1}$ for nPFK and dPFK, respectively. $K_{F6P}$ values in the absence of $F26P_2$ are 1.0 ± 0.1 mM for nPFK and 0.86 ± 0.06 mM for dPFK. In the presence of $F26P_2$, the $K_{F6P}$ value for nPFK decreases to 0.07 ± 0.02 mM, while that of dPFK decreases to 0.10 ± 0.01 mM.

Figure 7. A typical initial velocity pattern for *Ascaris suum* dPFK at pH 6.8, in 100 mM imidazole-HCl in the absence of $F26P_2$. The lines are the best fit of the data using eq 4, while the points are experimental values. Estimated kinetic parameters for all initial velocity patterns are discussed in the text.

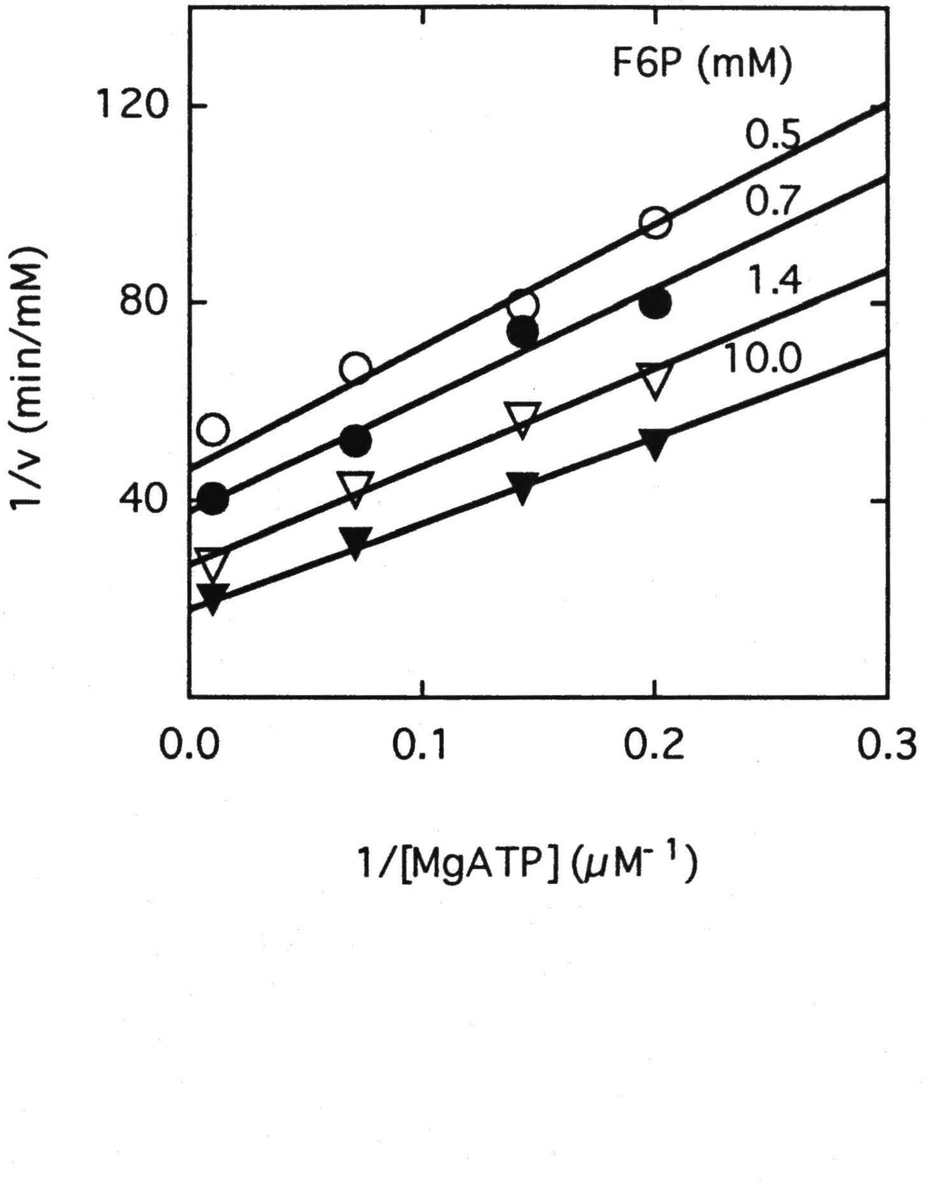
F6P (mM)
0.5
0.7
1.4
10.0
120
80
40
0.0
0.1
0.2
0.3
1/v (min/mM)
1/[MgATP] (μM⁻¹)

Figure 8. Dead-end inhibition by arabinose 5-phosphate of nPFK (pH 8.0) in the presence of 0.2 mM F26$P_2$. The lines are the best fit of the nPFK data using eq 5, while the points are experimental values.

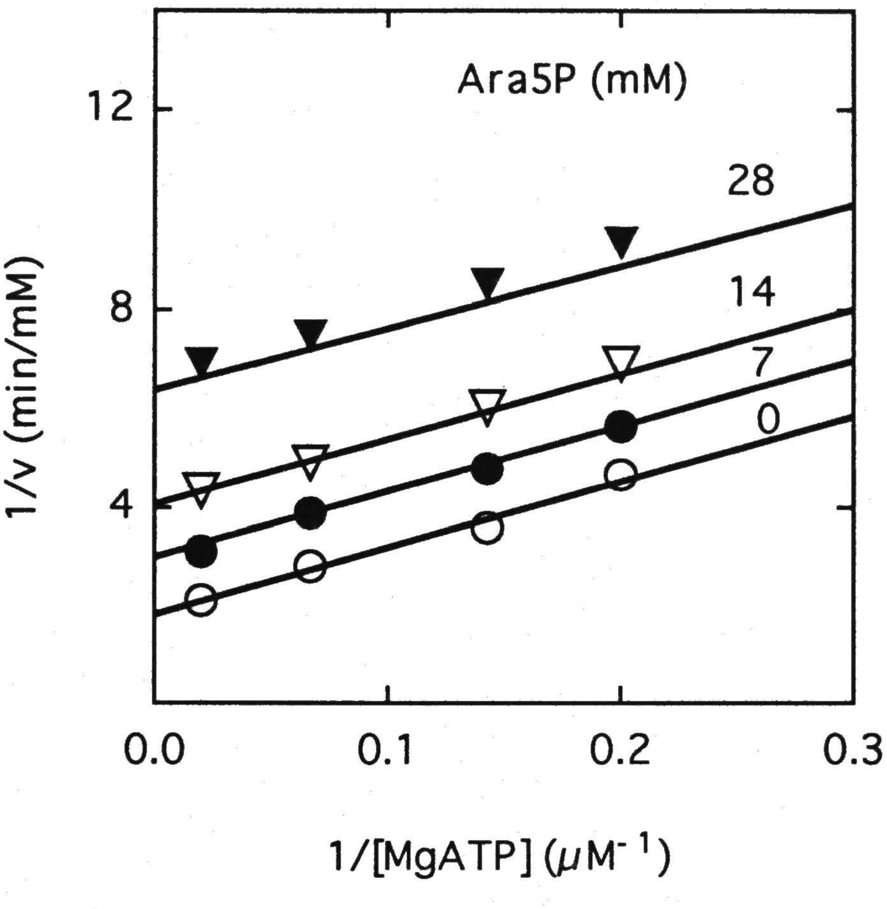
Ara5P (mM)
28
14
7
0
12
8
4
1/v (min/mM)
0.0
0.1
0.2
0.3
1/[MgATP] ($\mu$M$^{-1}$)

Figure 9. Dead-end inhibition by arabinose 5-phosphate of dPFK (pH 6.8) in the presence of 0.2 mM $F26P_2$. The lines are the best fit of the dPFK data using eq 6, while the points are experimental values.

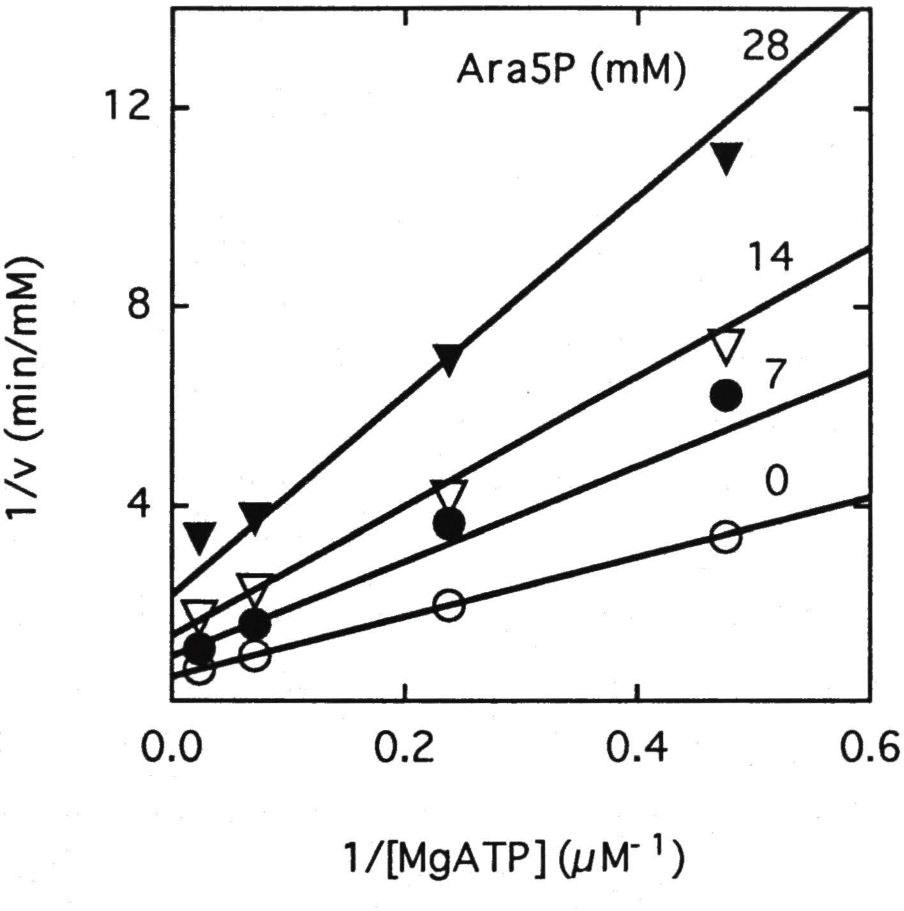
Ara5P (mM)
28
14
7
0
12
8
4
1/v (min/mM)
0.0
0.2
0.4
0.6
1/[MgATP] (μM⁻¹)

# CHAPTER IV

# ISOTOPE PARTITIONING AND INITIAL VELOCITY STUDIES WITH PHOSPHOFRUCTOKINASE AT VARIED $[Mg^{2+}]_{free}$

All of the initial velocity and isotope partitioning experiments with *A. suum* phosphofructokinase in the previous chapter were carried out at 8 mM total $Mg^{2+}$ in order to ensure that all ATP in a given experiment is present as the MgATP complex. However, it has been observed in this laboratory that the initial rate of the PFK reaction is faster at high (8.0 mM) than at low (1.0 mM) $Mg^{2+}$. The observation suggests that $Mg^{2+}$ may play a role in the reaction distinct from that of forming the MgATP chelate complex (unpublished observations). That $[Mg^{2+}]_{free}$ concentration might affect the catalytic activity of PFK is not unprecedented. Many enzymes catalyzing phosphoryl transfer reactions have been shown to require more than a single divalent metal ion for catalysis, including the catalytic subunit of cyclic AMP-dependent protein kinase (Cook *et al.*, 1982), choline kinase (Reinhardt *et al.*, 1984), pyrophosphatase (Knight *et al.*, 1984; Sosa *et al.*, 1992), sodium/potassium ATPase (Campos & Beauge, 1992), and pyrophosphate-dependent phosphofructokinase (Bertagnolli & Cook, 1994). Therefore, it is important to characterize the possible role of $Mg^{2+}$ in the *A. suum* PFK reaction. All experiments in this chapter were carried out with the dPFK at pH 6.8. Although subtle differences probably exist between the nPFK at pH 8.0 and the dPFK at pH 6.8, the basic mechanisms are the same for both enzymes (Rao *et al.*, 1987b; Rao *et al.*, 1991a).

*Initial Velocity Studies at Varied* $Mg^{2+}$. In order to determine whether the

steady state kinetic parameters, V, $K_{F6P}$, and $K_{MgATP}$, are affected by the concentration of $Mg^{2+}$, initial velocity experiments were carried out. The initial rate of the dPFK reaction was measured with F6P and MgATP concentrations fixed at their respective $K_m$ values while varying the total $Mg^{2+}$ concentration (Figure 10). The $Mg^{2+}$-dependence of the reaction velocity under these conditions appears to be biphasic, giving activation constants of approximately 15 μM and 200 μM. $Mg^{2+}$ appears to have a slight inhibitory effect at concentrations above 5 mM.

In order to analyze the details of the $Mg^{2+}$-activation, initial velocity patterns were obtained at several fixed concentrations of $Mg^{2+}$, correcting for metal-substrate complexes. Only the patterns at the lowest (0.1 mM) and highest (2.0 mM) $Mg^{2+}$ concentrations are shown (Figures 11 and 12). The pattern at low $Mg^{2+}$ is clearly intersecting while the pattern at high $Mg^{2+}$ is parallel. The parallel pattern is likely due to a low $K_D/K_m$ ratio for MgATP, and the qualitative difference between the two patterns is likely caused by $Mg^{2+}$ affecting this ratio. For patterns at 0.1, 0.2, 0.5, 1.0, and 2.0 mM $Mg^{2+}$, $V/K_{F6P}$ is essentially independent of the $Mg^{2+}$ concentration, while $V/K_{MgATP}$ increases about 4- to 5-fold from the lowest $Mg^{2+}$ concentration to the extrapolated saturating $Mg^{2+}$ concentration. The reciprocal of the increase in $V/K_{MgATP}$ versus the reciprocal of $Mg^{2+}$ concentration is linear (Figure 13), and a fit of the data using eq 3 gives an activation constant ($K_{act}$) for $Mg^{2+}$ of $0.31 \pm 0.07$ mM.

Since there is essentially no change in $K_{F6P}$ with $Mg^{2+}$ concentration, the assay system can be simplified by fixing F6P at a saturating concentration, and varying the $Mg^{2+}$ concentration at several different fixed concentrations of MgATP. The F6P concentration was fixed at 20 mM, while the MgATP concentration was varied from 10 to 500 μM and the $Mg^{2+}$ concentration was varied from 0.1 to 2.0 mM, as shown in Figure 14. A fit of the data using eq 7 gives a $K_{MgATP}$ value of $19 \pm 2$ μM, and a $K_{iMg^{2+}}$ value of $0.47 \pm 0.08$ mM, both in agreement with previous data. The $Mg^{2+}$-independent value

Figure 10. The $Mg^{2+}$ activation pattern for dPFK at pH 6.8, in 100 mM imidazole-HCl in the absence of $F26P_2$. MgATP and F6P were fixed around their respective $K_m$ values, while the total $Mg^{2+}$ varied without correction for the metal-substrate complexes. The two lines are linear regressions of the data at the lowest 5 points and the highest 7 points for illustration of the biphasic slope.

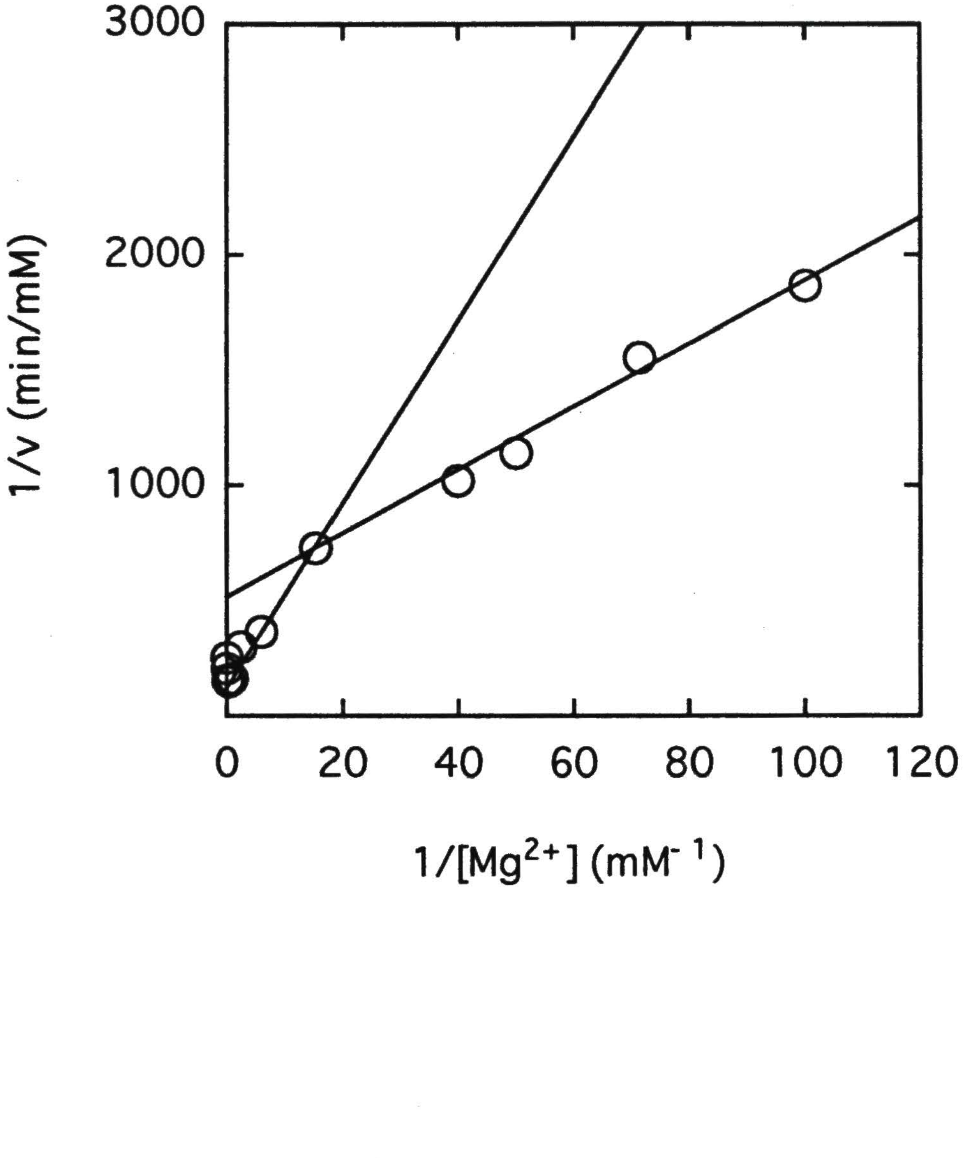
3000
2000
1000
1/v (min/mM)
0
20
40
60
80
100
120
1/[Mg$^{2+}$] (mM$^{-1}$)

Figure 11. Initial velocity pattern for dPFK at 0.1 mM $Mg^{2+}$. The $Mg^{2+}$ concentration was corrected for the metal-substrate complexes as described in Chapter II. The lines are the best fit to eq 4 while the points are experimental values. The symbols represent 1.0 mM F6P (open circles), 1.43 mM F6P (filled circles), 2.50 mM F6P (open triangles), and 10.0 mM F6P (filled triangles).

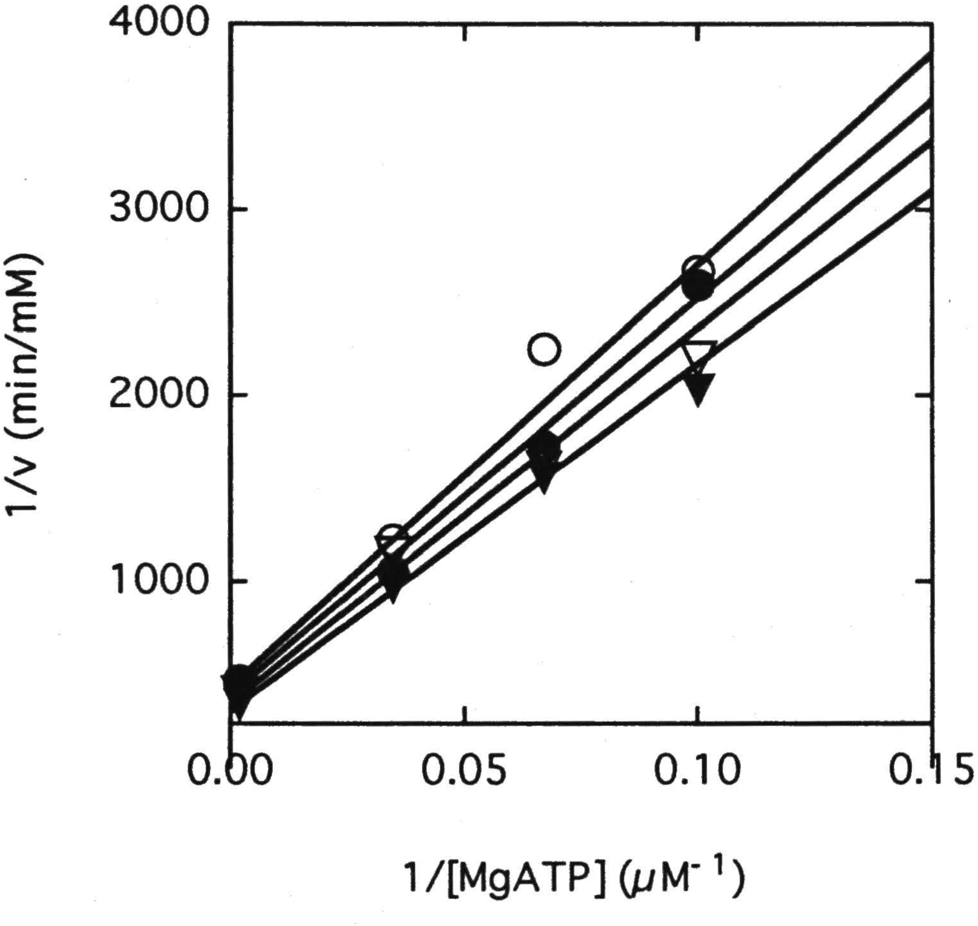
4000
3000
2000
1000
1/v (min/mM)
0.00
0.05
0.10
0.15
1/[MgATP] ($\mu$M$^{-1}$)

Figure 12. Initial velocity pattern for dPFK at 2.0 mM $Mg^{2+}$. The $Mg^{2+}$ concentration was corrected for the metal-substrate complexes as described in the text. The lines are the best fit with eq 4 while the points are experimental values. The symbols represent 1.0 mM F6P (open circles), 1.43 mM F6P (filled circles), 2.50 mM F6P (open triangles), and 10.0 mM F6P (filled triangles).

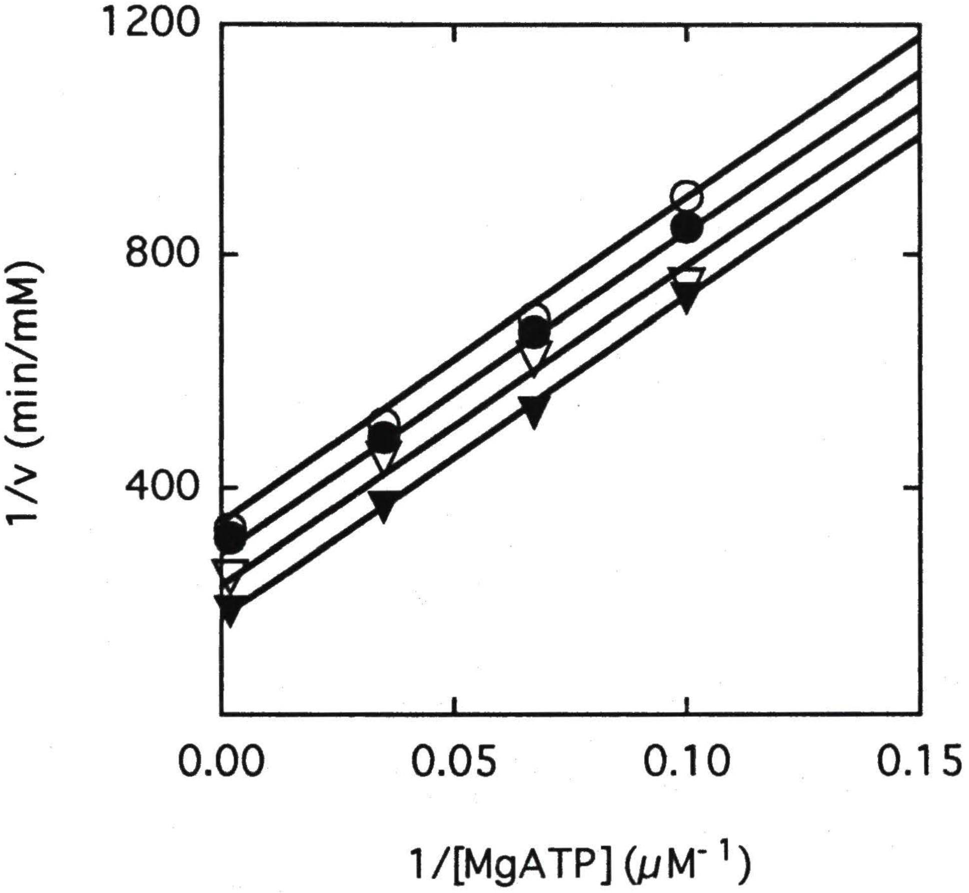
1200
800
400
1/v (min/mM)
0.00
0.05
0.10
0.15
1/[MgATP] ($\mu$M$^{-1}$)

Figure 13. $K_{act}$ plot for $Mg^{2+}$ activation of dPFK (pH 6.8), showing the reciprocal of the $V/K_{MgATP}$ values obtained from initial velocity patterns (including Figures 11 and 12) at different $Mg^{2+}$ concentrations versus the reciprocal of the $Mg^{2+}$ concentration. The data are fitted to eq 3, where v and V are substituted by $V/K_{MgATP}$ and $(V/K_{MgATP})_{max}$, A is the $Mg^{2+}$ concentration, and $K_a$ is $K_{act}$ for $Mg^{2+}$.

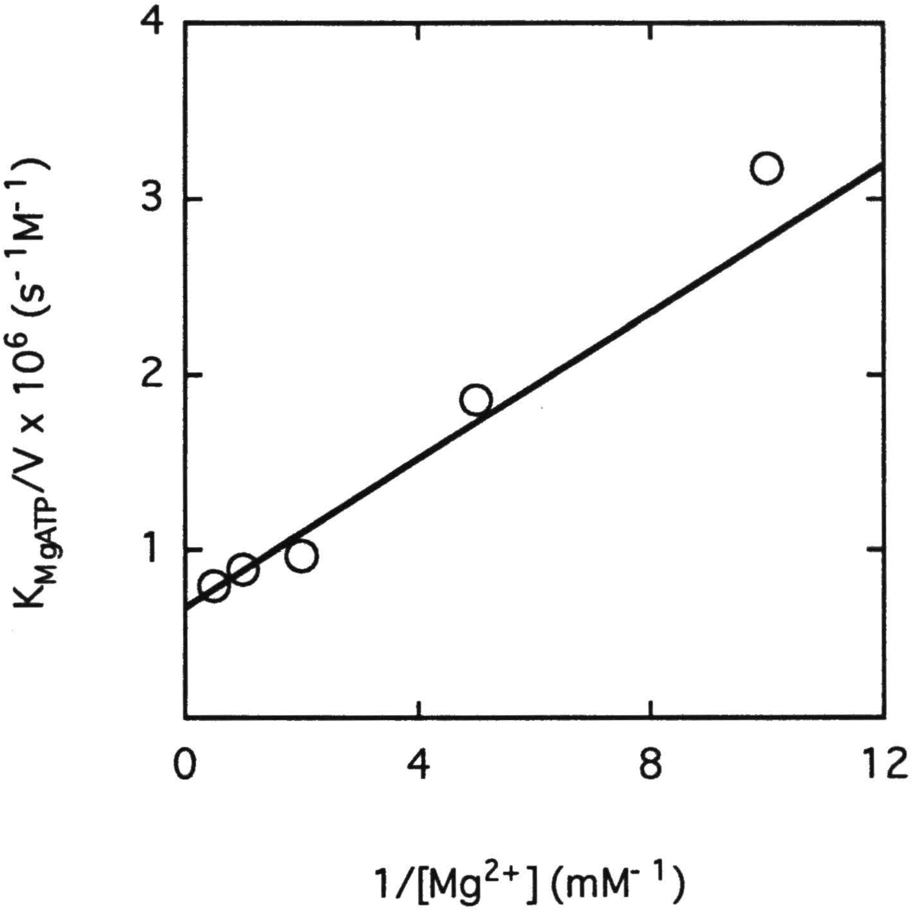
$K_{MgATP}/V \times 10^6$ ($s^{-1}M^{-1}$)
4
3
2
1
0
4
8
12
$1/[Mg^{2+}]$ ($mM^{-1}$)

Figure 14. Initial velocity pattern varying MgATP and $Mg^{2+}$ with F6P fixed at saturating. The lines are the best fit of the data with eq 7, while the points are experimental values. The symbols represent 0.1 mM $Mg^{2+}$ (open circles), 0.2 mM $Mg^{2+}$ (filled circles), 0.5 mM $Mg^{2+}$ (open triangles), 1.0 mM $Mg^{2+}$ (filled triangles), and 2.0 mM $Mg^{2+}$ (open squares).

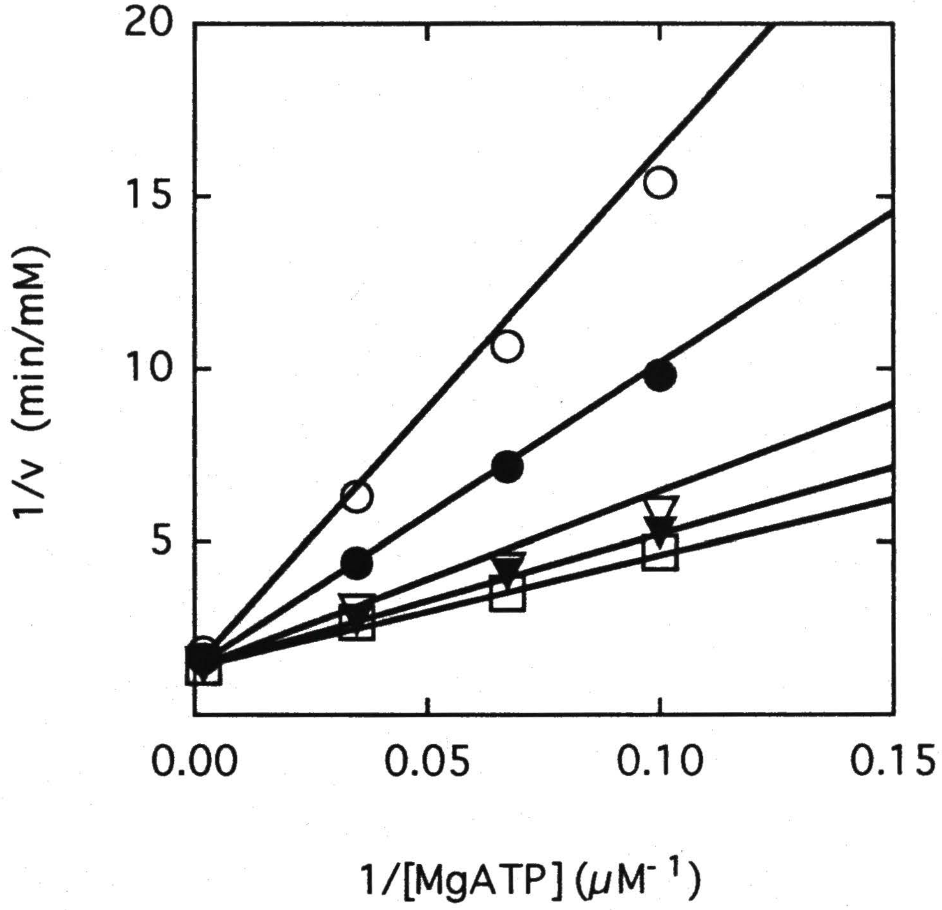
20
15
10
5
0.00
0.05
0.10
0.15
1/v (min/mM)
1/[MgATP] ($\mu$M$^{-1}$)

of $V/E_t$ from Figure 14 is 38 ± 2 $s^{-1}$, Table 2. A $V/E_t$ value of 36 ± 3 $s^{-1}$ is obtained in the presence of $F26P_2$ (Figure 15), which is within error equal to the value obtained in the absence of $F26P_2$. The corresponding $K_{F6P}$ values in the absence and presence of $F26P_2$ are 0.49 ± 0.07 mM and 0.15 ± 0.01 mM, respectively (Table 2).

*$K_D$ Determination.* As described in Chapter III, an isotope partitioning experiment requires that the dissociation constant for the enzyme:substrate complex is known. Although the initial velocity patterns obtained at 2.0 mM (Figure 12) or higher $Mg^{2+}$ give near-parallel lines with undefined $K_{iMgATP}$ values, the pattern at 0.1 mM $Mg^{2+}$ (Figure 11) shows intersecting lines and gives an estimated $K_{iMgATP}$ value of 30 ± 15 μM. The low $Mg^{2+}$ pattern in the presence of $F26P_2$ is shown in Figure 15 and gives a $K_{iMgATP}$ value of 38 ± 10 μM, within error equal to that obtained in the absence of $F26P_2$.

*Isotope Partitioning of dPFK:MgATP* in the Absence or Presence of $F26P_2$.* The isotope partitioning of the dPFK:MgATP complex at 0.1 mM $Mg^{2+}$ in the presence or absence of $F26P_2$ is shown in Figure 16. In both cases, a $P^*_{max}$ of 16 ± 1 μM is obtained, representing 20 % of the MgATP bound in the initial binary complex, using dissociation constants of 30 ± 15 μM and 38 ± 10 μM for the dPFK:MgATP complex in the absence and presence of $F26P_2$, respectively. In the absence of $F26P_2$, a $K'_{F6P}$ value of 0.66 ± 0.05 mM is obtained, while in the presence of $F26P_2$ the value decreases by about 8-fold to 0.08 ± 0.01 mM. Data are summarized in Table 2.

The isotope partitioning of the dPFK:MgATP* complex at 5 mM $Mg^{2+}$ in the presence or absence of $F26P_2$ is also shown in Figure 16. The results are similar to those obtained in Chapter III (Table 1), giving $P^*_{max}$ values of 93 μM and 67 μM in the absence and presence of $F26P_2$, respectively, representing 95% and 68% of the MgATP* bound in the initial binary complex. The corresponding $K'_{F6P}$ values are 0.76 mM and

Table 2. Summary of Data from Isotope Partitioning of
dPFK:MgATP* at Low and High[c] $Mg^{2+}$

| | 5 mM $Mg^{2+}$ | | 0.1 mM $Mg^{2+}$ | |
|---|---|---|---|---|
| | $-F26P_2$ | $+F26P_2$ | $-F26P_2$ | $+F26P_2$ |
| $V/E_t$ ($s^{-1}$) | 38 ± 2 | 36 ± 3 | 38 ± 2 | 36 ± 3 |
| $K_{F6P}$ (mM)[a] | 1.2 ± 0.1 | 0.13 ± 0.01 | 0.49 ± 0.07 | 0.15 ± 0.01 |
| $K_{iMgATP}$ (μM)[b] | 2.0 ± 0.5 | 2.3 ± 0.7 | 30 ± 15 | 38 ± 10 |
| $P^*_{max}$ (μM) | 93[c] (95%) | 67 (68%) | 16 ± 1 (20 ± 1%) | 16 ± 1 (20 ± 1%) |
| $K'_{F6P}$ (mM) | 0.76 | 0.15 | 0.66 ± 0.05 | 0.08 ± 0.01 |
| $[E{:}A]_0/P^*_{max}$ | 1.05 ± 0.10 | 1.47 ± 0.12 | 5.0 ± 0.5 | 5.0 ± 0.5 |
| $k_{off}$ ($s^{-1}$) | 25 ± 7 | 44 ± 9 | 48 ± 12 | 19 ± 5 |
| | - | to 64 ± 12 | to 240 ± 60 | to 100 ± 25 |
| $k_7/k'_5$ | - | 0.50 | 4.0 ± 0.3 | 4.0 ± 0.3 |
| $k_7$ ($s^{-1}$) | - | 18 ± 2 | 145 ± 5 | 145 ± 5 |
| $k_{on}$ ($M^{-1}s^{-1}$) | $(1.3 \pm 0.5) \times 10^7$ | $(1.9 \pm 0.8) \times 10^7$ | $(1.6 \pm 0.9) \times 10^6$ | $(6.3 \pm 3.2) \times 10^5$ |
| | | to $(2.8 \pm 1.4) \times 10^8$ | to $(8.1 \pm 3.9) \times 10^6$ | to $(3.2 \pm 1.4) \times 10^6$ |

[a] All $K_{F6P}$ values were determined using the single aldolase/triosephosphate isomerase/α-glycerolphosphate dehydrogenase coupled assay with coupling enzyme solutions made fresh from lyophilized powder to avoid the affects of $(NH_4)_2SO_4$ on $K_{F6P}$.

[b] For data at 5 mM $Mg^{2+}$, $K_{iMgATP}$ was calculated from the CD studies; for data at 0.1 mM $Mg^{2+}$, $K_{iMgATP}$ was obtained as an estimate from a computer fit of eq 4 to the initial velocity data.

[c] Partitioning data at 5 mM $Mg^{2+}$ were obtained as a repeat of the high $Mg^{2+}$ data for dPFK (shown in Table 1) using the same enzyme preparation that was used in experiments at 0.1 mM $Mg^{2+}$. This was to ensure that apparent $Mg^{2+}$ effects on isotope partitioning parameters were not caused by changes in the enzyme preparations. Only two points were measured for each of the ± $F26P_2$ experiments, so no error estimates were obtained from a fit to the data.

Figure 15. Initial velocity pattern for dPFK at 0.1 mM $Mg^{2+}$ in the presence of 0.2 mM $F26P_2$. The lines are the best fit of the data using eq 4, while the points are experimental values. The symbols represent 0.100 mM F6P (open circles), 0.143 mM F6P (filled circles), 0.250 mM F6P (open triangles), and 1.00 mM F6P (filled triangles).

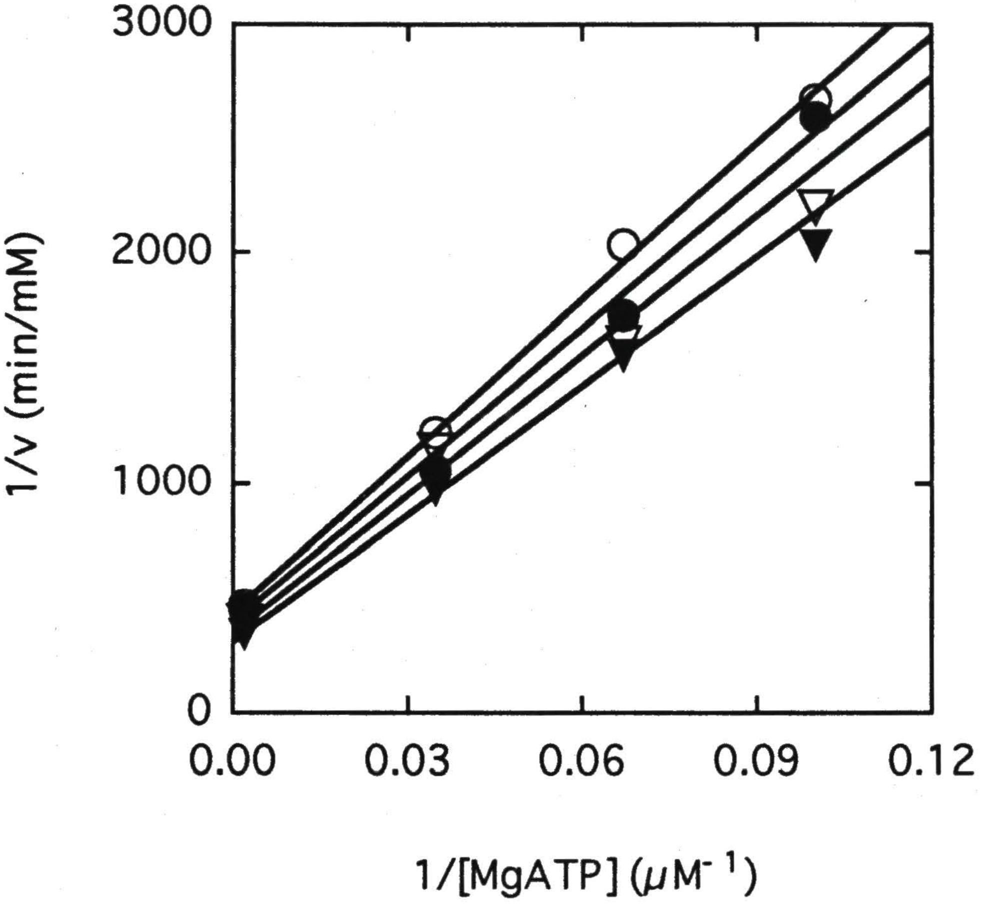
3000
2000
1000
0
1/v (min/mM)
0.00
0.03
0.06
0.09
0.12
1/[MgATP] (μM⁻¹)

Figure 16. Isotope trapping of the dPFK:MgATP* complex at 0.1 mM (triangles) and 5.0 (circles) $Mg^{2+}$ in the absence (open symbols) and presence (filled symbols) of 0.2 mM $F26P_2$. The amount of [1-$^{32}$P]FBP formed at different concentrations of F6P in the chase solution was determined as described in the text. The lines are the best fit of the data using eq 3, while the points are experimental values.

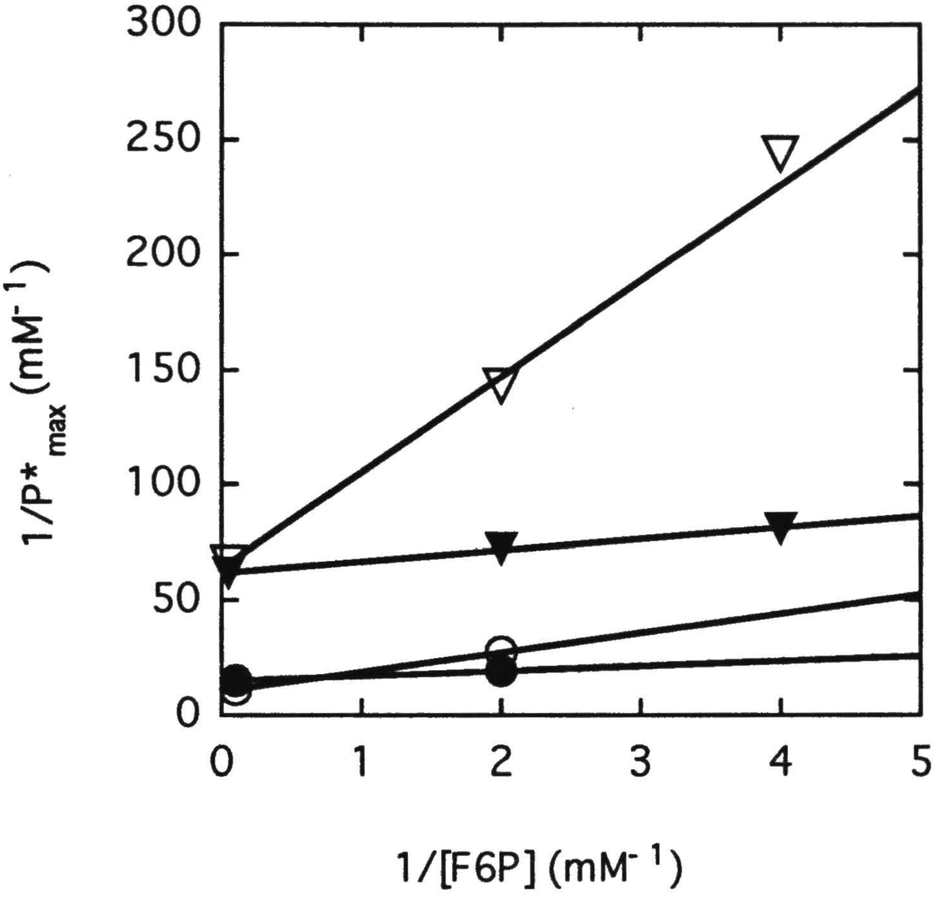
300
250
200
150
100
50
0
0
1
2
3
4
5
$1/P^*_{max}$ (mM$^{-1}$)
1/[F6P] (mM$^{-1}$)

0.15 mM, respectively. Data are summarized in Table 2.

*Arabinose 5-Phosphate Inhibition.* The arabinose 5-phosphate (Ara5P) versus MgATP inhibition patterns for dPFK in the absence and presence of $F26P_2$ are shown in Figures 17 and 18, respectively. The data adhere to noncompetitive inhibition for both inhibition patterns. In the absence of $F26P_2$, a fit of the data using eq 6 gives a $K_{MgATP}$ of 33 ± 2 μM, a $K_{is}$ of 23 ± 6 mM, and a $K_{ii}$ of 5.0 ± 0.3 mM. In the presence of $F26P_2$, a fit of the data using eq 6 yields a $K_{MgATP}$ of 34 ± 2 μM, a $K_{is}$ of 7 ± 1 mM, and a $K_{ii}$ of 8 ± 1 mM.

Figure 17. Dead-end inhibition by arabinose 5-phosphate of dPFK (pH 6.8) at 0.1 mM $Mg^{2+}$ in the absence of $F26P_2$. The lines are the best fit of the dPFK data using eq 6, while the points are experimental values.

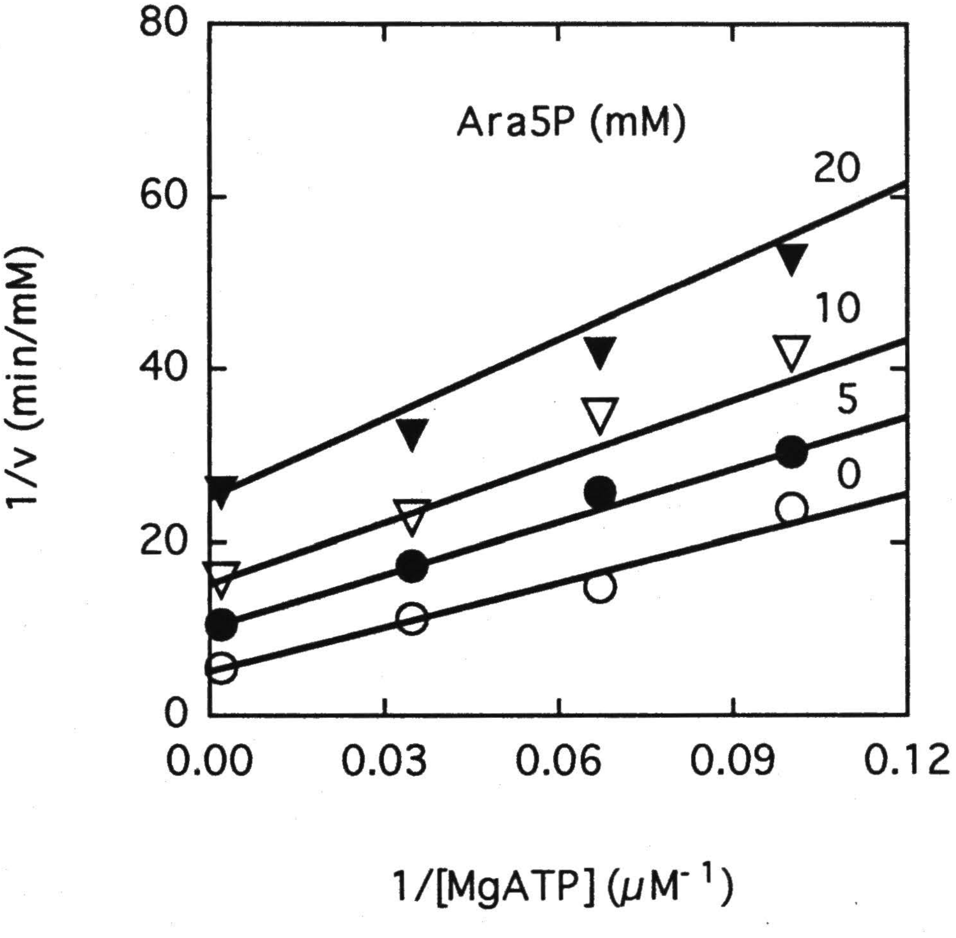
Ara5P (mM)
20
10
5
0
1/v (min/mM)
0
20
40
60
80
0.00
0.03
0.06
0.09
0.12
1/[MgATP] ($\mu$M$^{-1}$)

Figure 18. Dead-end inhibition by arabinose 5-phosphate of dPFK (pH 6.8) at 0.1 mM $Mg^{2+}$ in the presence of $F26P_2$. The lines are the best fit of the dPFK data using eq 6, while the points are experimental values.

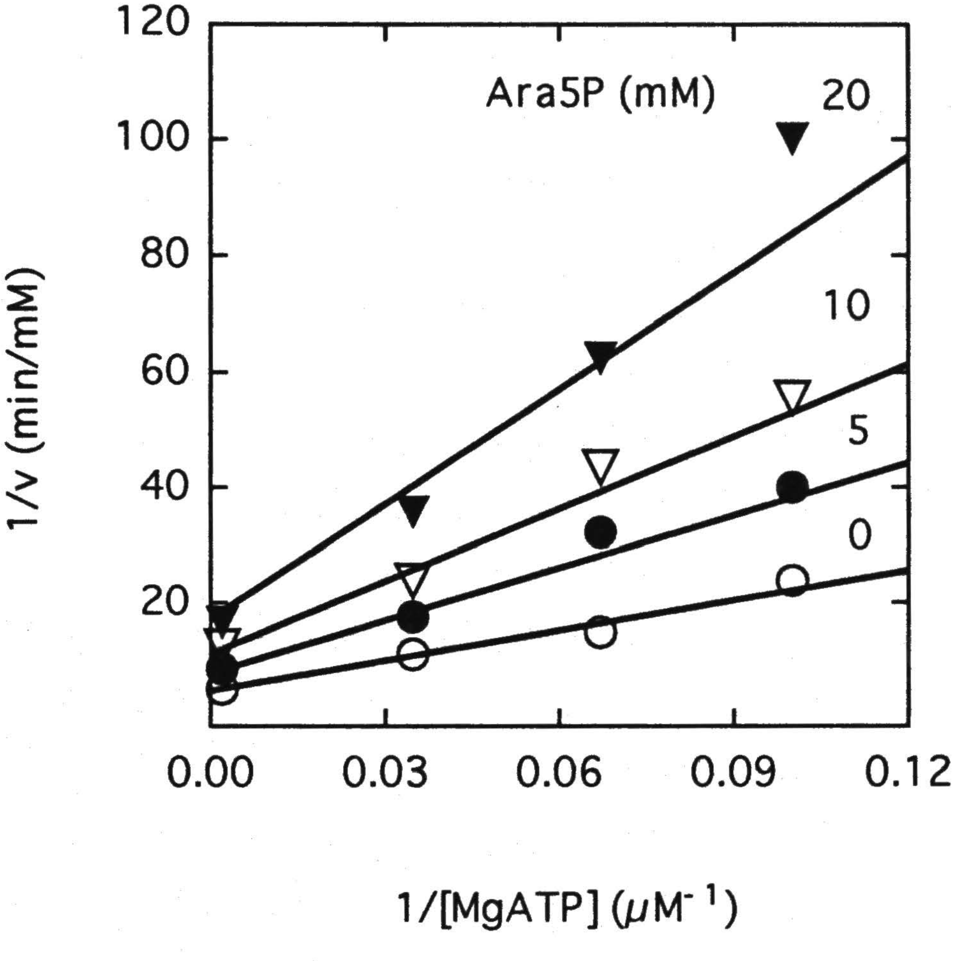
120
100
80
60
40
20
1/v (min/mM)
Ara5P (mM)
20
10
5
0
0.00
0.03
0.06
0.09
0.12
1/[MgATP] (μM⁻¹)

# CHAPTER V

# DISCUSSION

For the concentrations of MgATP used in studying the *A. suum* PFK reaction, less than 0.5 mM, a total $Mg^{2+}$ concentration of 1 mM ensures that essentially 100% of the ATP in a reaction mixture is present as MgATP. All previous kinetic data including the data in Chapter III were obtained at the arbitrarily high $Mg^{2+}$ concentration of 8 mM on the assumption that the metal ion is necessary only in forming the MgATP complex. However, it has been observed in this laboratory that the rate of the PFK reaction is faster at 8 mM than at 1 mM total $Mg^{2+}$, a phenomenon that cannot be explained simply by a difference in the concentration of the substrate MgATP at the two levels of $Mg^{2+}$. The latter finding suggests an activating effect of $Mg^{2+}$ on *A. suum* PFK, and has led to the experiments at varied $Mg^{2+}$ described in Chapter IV. In the current chapter, data obtained at high $Mg^{2+}$ are discussed separately from the data obtained at varied $Mg^{2+}$. The data are then discussed in terms of the activating effects of $F26P_2$ and $Mg^{2+}$.

*Isotope Partitioning at High* $Mg^{2+}$ *in the Absence of* $F26P_2$. With nPFK, 94% of the estimated E:MgATP* complex was trapped and converted to product. The specific activity of the nPFK used in these experiments was 43 U/mg, or only 86% of the specific activity reported by Starling *et al.* (1982) for *Ascaris* PFK. The lower specific activity for the nPFK used in these experiments is likely the result of the presence of contaminating impurities and/or an inactive fraction of the nPFK itself. About 85% of the calculated E:MgATP* complex is trapped with dPFK. The dPFK is prepared by diethylpyro-carbonate (DEPC) modification of the ATP allosteric site with the enzyme

active site protected from modification by bound F6P (Rao *et al.*, 1987a). The decrease in the specific activity of dPFK compared to nPFK from which it was prepared suggests inactivation of some of the enzyme during preparation. The inactivation is expected since the concentration of F6P cannot be maintained high enough to give complete saturation at the active site. An estimate of 80% is obtained for protection at the active site (Rao *et al.*, 1987a). Thus, for both nPFK and dPFK the actual concentration of the initial E:MgATP* complex is less than the estimated value based on the assumption that all protein is active enzyme. Taking into account the inactive enzyme in both the nPFK and the dPFK preparations, both enzyme forms trap very close to 100% of the E:MgATP* initially present. The data for both nPFK and dPFK are consistent with a predominantly steady-state ordered kinetic mechanism, in agreement with the initial velocity data obtained previously (Rao *et al.*, 1987b). However, even 100% trapping of the E:MgATP complex does not rule out the possibility of a random mechanism, but only suggests that catalysis is much faster than MgATP dissociation. Indeed, the fact that F6P alone protects the active site against DEPC modification suggests that a minor pathway in which F6P binds to enzyme prior to MgATP probably does exist. However, the high $K_D$ (50 - 60 mM) for the E:F6P complex estimated from the F6P protection against DEPC modification (Rao *et al.*, 1987a) compared to the low $K_D$ (2 µM) for the E:MgATP complex and the rate constants for dissociation of E:MgATP:F6P gives an essentially ordered mechanism.

The $K'_{F6P}$ values of 0.54 ± 0.09 mM and 0.85 ± 0.15 mM for nPFK and dPFK, respectively, allow the estimation of the off-rate of MgATP from the binary complex using eq 8 (Rose, 1980):

$$\left(\frac{K'_{F6P}}{K_{F6P}}\right)\left(\frac{V}{E_t}\right) < k_{off} < \left(\frac{K'_{F6P}}{K_{F6P}}\right)\left(\frac{V}{E_t}\right)\left(\frac{[E{:}MgATP^*]_0}{P^*_{max}}\right) \tag{8}$$

Assuming 100% trapping, for nPFK the estimated $k_{off}$ is about 34 ± 7 $s^{-1}$, and for dPFK $k_{off}$ is about 42 ± 8 $s^{-1}$, Table 1. Using the dissociation constant value of 2 µM for both enzyme forms, the net on-rate for MgATP to enzyme is on the order of $10^7$ $M^{-1}s^{-1}$, which is about 10- to 100-fold less than the diffusion rate of combination of a small molecule and a macromolecule (Fersht, 1977). The difference in the estimated on-rate and the known diffusion rate suggests the possibility of a structural isomerization occurring after MgATP binds to enzyme.

*Isotope Partitioning at High $Mg^{2+}$ in the Presence of $F26P_2$.* In the presence of 0.2 mM $F26P_2$, no change in the $P^*_{max}$ or $K'_{F6P}$ values for nPFK is observed, that is essentially 100% of the E:MgATP* complex is trapped. Data are consistent with an ordered mechanism, and the off-rate for MgATP from the E:MgATP complex is 370 ± 120 $s^{-1}$, about 10-fold higher than that estimated in the absence of $F26P_2$. However, in the presence of 0.2 mM $F26P_2$ the dPFK gives a decrease in $P^*_{max}$ to 54 % of that obtained in the absence of effectors. The $K'_{F6P}$ value for dPFK trapping in the presence of $F26P_2$ decreases by 3.3-fold from that obtained in the absence of effectors. The decrease in $P^*_{max}$ in the presence of $F26P_2$ suggests that some of the MgATP is able to dissociate from the ternary complex prior to catalysis. Using eq 8, the data for dPFK in the presence of $F26P_2$ give a $k_{off}$ range of 110 ± 30 to 200 ± 45 $s^{-1}$, 2.5- to 4-fold greater than the value in the absence of $F26P_2$. Assuming a dissociation constant of approximately 2 to 6 µM, the on-rates for both enzyme forms are again on the order of $10^7$ $M^{-1}s^{-1}$.

In the case of the dPFK where less than 100% trapping is estimated, the partition ratio, $k_7/k'_5$, Scheme I, can be calculated using eq 9:

$$\frac{k_7}{k'_5} = \frac{[\mathrm{E{:}MgATP^*}]_0}{P^*_{max}} - 1 \qquad (9)$$

**Scheme I.** Steps in the Substrate Trapping of MgATP* with PFK.

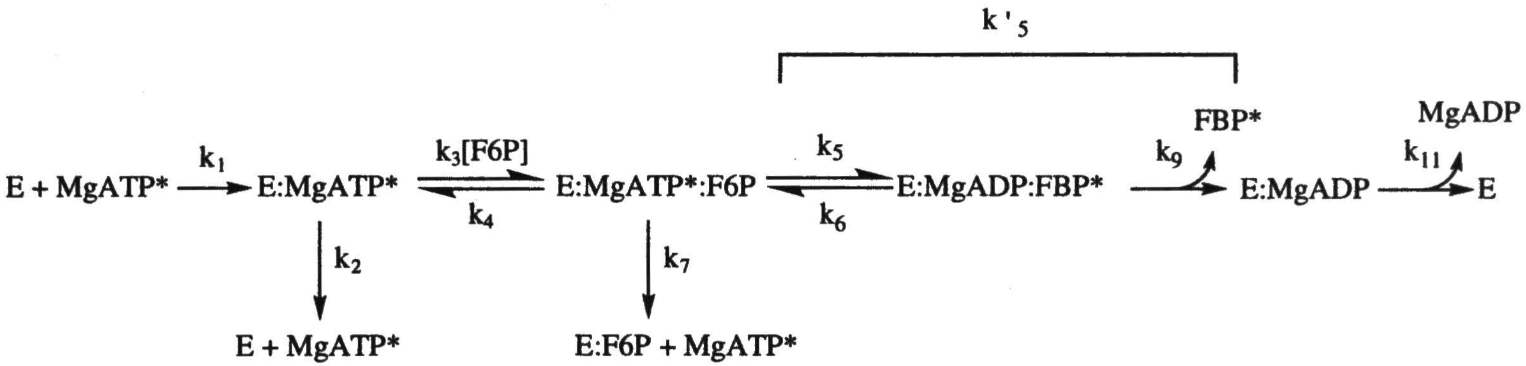
k'5
E + MgATP*
k1
E:MgATP*
k3[F6P]
k4
E:MgATP*:F6P
k5
k6
E:MgADP:FBP*
k9
FBP*
E:MgADP
k11
MgADP
E
k2
E + MgATP*
k7
E:F6P + MgATP*

$k'_5$ is the net rate constant for all steps involved in converting the E:MgATP:F6P complex to products and the release of the first product. The partition ratio is zero when 100% trapping occurs because $k_7$ is much smaller than $k'_5$. In order for only partial trapping to occur $k_7$ must be of the same order as $k'_5$, giving a partition ratio greater than zero. Thus, the increase in the partition ratio for dPFK in the presence of $F26P_2$ (see Table 1) must be caused either by nPFK having a much larger $k'_5$ with respect to $k_7$ than dPFK, or by dPFK having a much larger $k_7$ than nPFK in the presence of $F26P_2$. $k'_5$ is the same as $V/E_t$ (Table 1), and since the $V/E_t$ values for nPFK and dPFK are similar, the high partition ratio for dPFK is likely not due to large differences in $k'_5$ for nPFK and dPFK. So, the difference in the partition ratios between nPFK and dPFK in the presence of $F26P_2$ must be a result of dPFK having a much larger value for $k_7$ than nPFK. Such a 'leaky' ternary complex is consistent with a random kinetic mechanism for dPFK in the presence of $F26P_2$. Using a $k'_5$ value of $42 \pm 1$ $s^{-1}$ for dPFK, $k_7$ is estimated to be 36 $\pm 2$ $s^{-1}$. It should be pointed out that no trapping of the dPFK:$^{14}C$-F6P complex occurred, which lends support to a strictly ordered mechanism. However, the lack of trapping of F6P does not rule out a partially random mechanism but only suggests that either the E:F6P complex does not form (or has a $K_D$ much larger than the concentration of F6P used in the pulse solution), or that the off-rate for F6P is much faster than catalysis.

*Initial velocity studies at High $Mg^{2+}$.* Initial velocity studies also support the finding that $F26P_2$ shifts the kinetic mechanism for dPFK from ordered to random. The uncompetitive inhibition (Figure 8) by Ara5P versus MgATP in the presence of $F26P_2$, consistent with the isotope partitioning data and an ordered kinetic mechanism. The Ara5P versus MgATP inhibition pattern was also important in determining the kinetic mechanism of *A. suum* PFK in the absence of $F26P_2$ (Rao *et al.*, 1987b). The authors

showed uncompetitive inhibition patterns in the absence of $F26P_2$ for both nPFK and dPFK.

The typical initial velocity pattern for either nPFK or dPFK gives a series of near-parallel lines (Figure 7). A ping pong mechanism has previously been ruled out for *A. suum* PFK (Rao *et al.*, 1987b). The fact that radioactive product formation in the isotope partitioning experiments is dependent on the amount of chasing substrate (F6P) also rules out a ping pong mechanism. Any covalently bound enzyme intermediate that survives the brief pulse/chase time period would give a constant amount of trapping independent of the chasing substrate. The near-parallel lines in the initial velocity patterns are thus caused by the $K_D$ for the E:MgATP complex being much smaller than the $K_m$ for MgATP, and that the concentration of MgATP was varied around the $K_m$. The same near-parallel initial velocity pattern is seen with rabbit muscle PFK (Uyeda, 1970). It has been postulated with the rabbit enzyme that the pattern is not due to a ping pong mechanism but to a low $K_D/K_m$ ratio. The $K_D$'s calculated from the present circular dichroism studies confirm a low $K_D/K_m$ ratio for the *A. suum* PFK.

The fact that earlier initial velocity studies with *A. suum* PFK (Rao *et al.*, 1987b) in the absence of $F26P_2$ showed initial velocity patterns that clearly intersected and gave estimates of $K_D$ values similar to the $K_{MgATP}$ values for both nPFK and dPFK is ascribed to error in the earlier assays due to rapid consumption of MgATP and to low sensitivity of the assay (the slope effect was generated by the initial rates measured at the lowest concentration of MgATP). The earlier initial velocity patterns were measured using the single aldolase/triose phosphate isomerase/α-glycerolphosphate dehydrogenase coupled assay. The present study has avoided the problems of rapid loss of substrate and low sensitivity by using the double coupled assay which recycles the consumed MgATP via the pyruvate kinase reaction and gives a 1.5-fold greater sensitivity than the aldolase coupled assay alone.

*Initial Velocity Studies at Varied $Mg^{2+}$*. The $Mg^{2+}$ activation pattern shown in Figure 10 indicates a biphasic increase in the reaction velocity with increasing total $Mg^{2+}$, with activation constants of approximately 15 µM and 200 µM. Since the total $Mg^{2+}$ concentration in these assays was not corrected for the formation of the MgATP complex, the lower constant of 15 µM likely represents the titration of ATP to form the substrate MgATP. This value of 15 µM is in excellent agreement with the values of $K_{MgATP}$ reported in this dissertation and in previous publications (Payne *et al.*, 1991; Rao *et al.*, 1987b). The higher constant obtained from Figure 10 likely represents the formation of an $E{:}Mg^{2+}$ complex, where $Mg^{2+}$ is an activator of the enzyme.

The activation of PFK by $Mg^{2+}$ is more easily seen in the initial velocity patterns at low and high $Mg^{2+}$, Figures 11 and 12. The qualitative change from an intersecting pattern (Figure 11) to a parallel pattern (Figure 12) suggests a decrease in the $K_D/K_m$ ratio for MgATP when going from low to high $Mg^{2+}$. The decrease in $K_{iMgATP}$ at saturating $Mg^{2+}$ from that at 0.1 mM $Mg^{2+}$ is about 15-fold, from 30 µM to 2 µM, while the decrease in $K_{MgATP}$ over the same range is only about 3- to 4-fold. The total activation is realized in the parameter $V/K_{MgATP}$, and the dependence of this parameter on $Mg^{2+}$ is shown as a reciprocal plot in Figure 13. The $K_{act}$ for $Mg^{2+}$ obtained from Figure 13 is $0.31 \pm 0.07$ mM, in good agreement with the activation constant obtained from the steepest slope in Figure 10. The simplified $Mg^{2+}$ activation pattern shown in Figure 14 gives a smaller error in the estimate of $K_{act}$ than Figure 13 because of the higher velocities being measured (F6P is saturating) and because only one F6P concentration must be corrected for the formation of MgF6P. Figure 14 shows clearly that $Mg^{2+}$ has no effect on V and a fit of eq 7 to the data gives a $K_D$ for $Mg^{2+}$ of $0.47 \pm 0.08$ mM, in good agreement with the values of $K_{act}$ obtained from Figures 10 and 13. The data fit also gives a $K_{MgATP}$ of $19 \pm 2$ µM and a $V/K_{MgATP} \cdot E_t$ of $1.9 \times 10^6$ $M^{-1}s^{-1}$, both in excellent agreement with the values reported by Payne *et al.* (1995).

*Isotope Partitioning at Low $Mg^{2+}$*. The dPFK at 0.1 mM $Mg^{2+}$ in the absence or presence of $F26P_2$ is able to trap 16 μM of the MgATP* as product, which is only 20% of the MgATP* bound in the initial binary complex. The calculated partial trapping is likely not due to error in the estimation of the enzyme concentration or the dissociation constant for E:MgATP. The repeat of the isotope partitioning experiment at high $Mg^{2+}$ (5 mM) using the same enzyme preparation gave a maximum trapping value of 93 μM, or 95% of the MgATP* bound in the initial binary complex. As described in the discussion of the trapping at high $Mg^{2+}$, the trapping likely represents 100% of the E:MgATP* complex. The concentration of MgATP in the pulse is higher than the concentration of enzyme and much higher than the $K_D$ for the E:MgATP complex, so the concentration of E:MgATP is equivalent to the total enzyme concentration. Using 93 μM as the total enzyme concentration, the dissociation constant for the E:MgATP complex at 0.1 mM $Mg^{2+}$ would have to be about 25-fold higher than the estimated 30 μM in order for the maximal trapping of 16 μM to represent 100% trapping. The partial trapping at low $Mg^{2+}$ indicates that MgATP is able to dissociate from the ternary complex both in the presence or absence of $F26P_2$, consistent with a random mechanism.

As with the data for dPFK at high $Mg^{2+}$ in the presence of $F26P_2$, the Ara5P versus MgATP inhibition pattern confirms the randomness of the mechanism at low $Mg^{2+}$ both in the absence or presence of $F26P_2$. The inhibition patterns are noncompetitive, indicating that the F6P analog is able to bind to enzyme both before and after MgATP. Using eq 9, the 20% trapping at low $Mg^{2+}$ gives a partition ratio ($k_7/k'_5$) of 4, as shown in Table 2. Using the $V/E_t$ value of 36 - 38 $s^{-1}$ from Table 2 as the value of $k'_5$, the value of $k_7$ is 145 $s^{-1}$. The value of $k_7$ at high $Mg^{2+}$ in the absence of $F26P_2$ is essentially zero, while the value of $k_7$ at high $Mg^{2+}$ in the presence of $F26P_2$ is finite but 8-fold smaller than the $F26P_2$-independent value of $k_7$ obtained at low $Mg^{2+}$. The increase in the off-rate of MgATP from the ternary complex at low $Mg^{2+}$ is consistent

with the increase in the $K_D$ for the E:MgATP binary complex.

In the absence of $F26P_2$, the isotope trapping at 0.1 mM $Mg^{2+}$ gives a $K'_{F6P}$ of 0.66 ± 0.05 mM, which is comparable to the value of 0.85 ± 0.15 mM obtained for trapping at high $Mg^{2+}$ in the absence of effectors (Table 1). In the presence of $F26P_2$, the $K'_{F6P}$ value decreases to 0.08 ± 0.01 mM, which is about 3-fold less than the value of 0.26 ± 0.07 mM obtained for $K'_{F6P}$ at high $Mg^{2+}$. The $K'_{F6P}$ value obtained at low $Mg^{2+}$ in the presence of $F26P_2$ is also about 8-fold less than that obtained in the absence of $F26P_2$. Using eq 8, the value for $k_{off}$ is in the range of 48 ± 12 to 240 ± 60 $s^{-1}$ in the absence of $F26P_2$ and 19 ± 5 to 100 ± 25 $s^{-1}$ in the presence $F26P_2$. Using a dissociation constant of 30 to 38 μM for the E:MgATP complex both in the absence and presence of $F26P_2$, the on-rate is on the order of $10^6$ $M^{-1}s^{-1}$, which is at least 100-fold slower than the estimated diffusion rate.

*Structural Isomerization of the E:MgATP Complex.* As mentioned, there is good evidence for an isomerization of E:MgATP. First, changes are observed in the far UV CD spectrum of PFK upon binding of MgATP. Second, the $V/(K_{MgATP} \cdot E_t)$ is pH-independent and equal to 1.4 x $10^6$ $M^{-1}s^{-1}$ (Payne *et al.*, 1995). The V/K for the first reactant in an ordered mechanism is the on-rate for that reactant binding to enzyme, yet the value of $10^6$ $M^{-1}s^{-1}$ is significantly lower than the diffusion limit, consistent with a multi-step process for MgATP binding. Finally, the off-rate ($k_{off}$) for MgATP from enzyme that is estimated from the isotope partitioning studies at high $Mg^{2+}$ increases in the presence of $F26P_2$ while the $K_D$ for E:MgATP does not show any significant change, giving a net on-rate on the order of $10^7$ $M^{-1}s^{-1}$. Since it is unlikely that the rate of diffusion of MgATP to E ($k_1$) changes, other steps which limit the net on-rate must be involved in forming the E:MgATP active complex. Scheme I can be expanded to include an isomerization of the E:MgATP complex, Scheme II. Thus, the experimental $k_{off}$ is a

**Scheme II.** Kinetic Mechanism of *Ascaris suum* PFK.

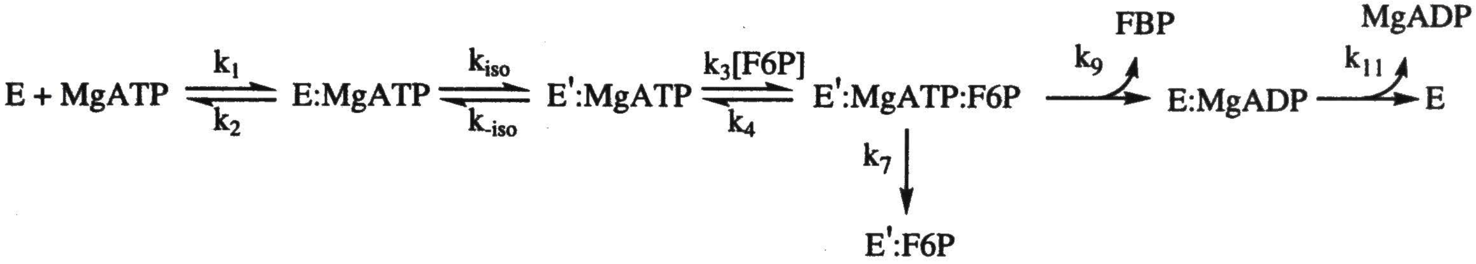
E + MgATP
k1
k2
E:MgATP
kiso
k-iso
E':MgATP
k3[F6P]
k4
E':MgATP:F6P
k7
E':F6P
k9
FBP
E:MgADP
k11
MgADP
E

net off-rate given by equation 10. Expressions for the $V/(K_{MgATP} \cdot E_t)$ and the observed $K_D$ for E′:MgATP are given by eqs. 11 and 12.

$$k_{off} = \frac{k_2 k_{-iso}}{k_2 + k_{iso}} \tag{10}$$

$$\frac{V}{K_{MgATP} \cdot E_t} = \frac{k_1 k_{iso}}{k_2 + k_{iso}} \tag{11}$$

$$K_D = \left(\frac{k_{-iso}}{k_{iso}}\right)\left(\frac{k_2}{k_1}\right) \tag{12}$$

$V/(K_{MgATP} \cdot E_t)$ represents the net on-rate for MgATP to form the isomerized (active) complex. Under conditions for obtaining $V/(K_{MgATP} \cdot E_t)$, saturating F6P, the isomerization step is irreversible. $K_D$ is the overall dissociation constant for the isomerized E′:MgATP complex. Limits can be placed on the isomerization rate constants. The constant $k_{iso}$ must be greater than or equal to the turnover number for formation of FBP (42 $s^{-1}$) and $k_{-iso}$ must be greater than or equal to the experimentally determined $k_{off}$, Tables 1 and 2. Finally, for 100% trapping to occur, either $k_{iso}$ must be greater than $k_{-iso}$ so that all bound MgATP is in the active isomerized form, or $k_{iso}$ must be greater than $k_2$ so that any non-isomerized E:MgATP will proceed toward product prior to dissociating. It is unlikely that $k_{iso}$ will be much greater than $k_2$, the diffusion-limited off-rate for MgATP. More likely is that $k_{iso}>k_{-iso}$, so that enzyme is predominantly E′:MgATP once MgATP binds. Thus for all of the conditions studied, the presence of $F26P_2$ likely increases the rate of the isomerization step so that if it were partially limiting in the absence of $F26P_2$, it no longer limits in the presence of the effector.

*Effects of $F26P_2$ on the PFK-Catalyzed Reaction.* The role of $F26P_2$ on the

isomerization of the binary complex is consistent with the role proposed by Payne *et al.* (1991; 1995) for $F26P_2$ in F6P binding. These authors have suggested that binding of $F26P_2$ to its allosteric site decreases the off-rate for F6P, presumably by facilitating isomerization of the ternary complex to its catalytically optimal conformation. The conclusion that $F26P_2$ decreases the off-rate for F6P is based on the fact that this effector lowers $K_{F6P}$ without affecting V. $K_{F6P}$ is defined by eq 13,

$$K_{F6P} = K_{iF6P}\left(\frac{1 + C_r + C_f}{1 + C_r + C_{vf}}\right) \tag{13}$$

where $K_{iF6P}$ is the dissociation constant for F6P, $C_f$ and $C_r$ are the commitment factors for the forward and reverse reactions, respectively, and $C_{vf}$ is the catalytic ratio for the forward reaction. As seen in eq 13, $F26P_2$ can decrease $K_{F6P}$ by affecting either the enzyme affinity for F6P ($K_{iF6P}$) or the complex kinetic constants, $C_f$ and $C_{vf}$. The kinetic data reported by Rao *et al.* (1987b) indicate that product release is fast, and thus V represents a net rate constant for the catalytic steps. Therefore, the lack of any effect by $F26P_2$ on V rules out an effect on the catalytic steps ($k'_5 = k_5$), and points to an effect only on the affinity for F6P. Assuming that the on-rate for F6P is diffusion-limited and cannot increase, the off-rate for F6P must decrease. The current isotope partitioning data at low $Mg^{2+}$ also support the conclusion that $F26P_2$ decreases the off-rate for F6P and does not affect the catalytic steps. At low $Mg^{2+}$ only partial trapping ($P^*_{max} < 100\%$) of the E:MgATP* complex occurs, and $P^*_{max}$ is $F26P_2$-independent. The extent of trapping is determined by the partition ratio, $k_7/k'_5$, and assuming that the release of first product, FBP, is not rate-limiting, an increase in the rate of turnover of the central complex ($k'_5$) should cause an increase in $P^*_{max}$. Since $P^*_{max}$ is not affected by the

presence of $F26P_2$ at low $Mg^{2+}$, it can be concluded that the catalytic steps are not affected by $F26P_2$. Thus, the above-mentioned data are consistent with $F26P_2$ decreasing the off-rate for F6P.

Recent data require that another possibility be considered. The less active oPFK exhibits an increase in V in the presence of $F26P_2$ while $K_{F6P}$ is not affected (unpublished observations by G. S. J. Rao in this lab). Thus, it is possible that $F26P_2$ increases the rate of interconversion of central complexes but that this increase is masked by other rate limiting steps, such as product release. Only in the case of oPFK, where the rate of interconversion of central complexes has become the slow step, is the effect of $F26P_2$ on V observed. Other evidence that $F26P_2$ affects the catalytic steps and not $K_{iF6P}$ comes from the Ara5P inhibition patterns. Ara5P is an inhibitory analog of F6P, and yet the $K_i$ for this inhibitor in the presence of $F26P_2$ (10-12 mM) is not significantly different from the $K_i$ reported by Rao *et al.* (1987b) for inhibition in the absence of $F26P_2$. Assuming that Ara5P is a reasonably good analog of F6P, the dissociation constant for F6P must also be $F26P_2$-independent. Thus, the oPFK and Ara5P data suggest that $F26P_2$ does not affect the enzyme affinity for F6P, but increases the rate of the catalytic steps.

It is possible that the previous conclusion that $F26P_2$ only affects the off-rate for F6P was based on an incorrect assumption that the release of the product, FBP or MgADP, does not limit the forward reaction rate. The assumption that the release of FBP is very fast is based on product inhibition by FBP, which is uncompetitive versus MgATP and competitive versus F6P, suggesting that FBP does not bind to the E:MgADP complex but forms the E:MgATP:FBP dead-end complex. That the E:MgADP complex has essentially no affinity for FBP is consistent with very fast release of FBP, as concluded by Payne *et al.* (1991) and Rao *et al.* (1987). However, if the release of MgADP from enzyme is very fast, then essentially no E:MgADP exists in the steady-

state. Thus, the lack of binding of FBP to E:MgADP may not be because of a very fast off-rate for FBP, but because no E:MgADP is present.

The question of whether or not the release of FBP is fast compared to the catalytic steps can be answered experimentally using the technique of positional isotope exchange (PIX; Mullins & Raushel, 1995). The technique uses $^{31}P$ nuclear magnetic resonance (NMR) and the fact that the chemical shift of the $\gamma$-phosphate is slightly different when directly bound to $^{18}O$ than when directly bound to $^{16}O$. The substrate MgATP is first labeled with $^{18}O$ at the bridge position between the $\beta$- and $\gamma$-phosphates. The $^{31}P$ NMR chemical shift of the $\gamma$-phosphate of the bridge-labeled MgATP is then measured during catalytic turnover. If any reversible steps occur during the catalytic steps prior to product release, then a scrambling of [$^{18}O$]bridge-labeled ATP occurs due to free rotation of the $\beta$-phosphate of MgADP. Such a scrambling of the bridge oxygen causes a decrease in the $^{31}P$ signal for the $\gamma$-phosphate directly bound to $^{18}O$, and an increase in the $^{31}P$ signal for the $\gamma$-phosphate directly bound to $^{16}O$. If release of FBP is fast compared to the catalytic steps, then no such reversibility is possible, and thus no change in the $\gamma$-phosphate signal occurs.

If the release of FBP is indeed rate-limiting, then the kinetic and isotope partitioning data must be analyzed using eq 13. Note that the numerator and denominator in parenthesis differ only by the terms $C_f$ and $C_{vf}$. The forward commitment factor, $C_f$, is defined as $k_5/k_4$, the ratio of the rate of the catalytic step to the rate of dissociation of the ternary complex, while the catalytic ratio, $C_{vf}$, is defined as $k_5/k_{iso} + k_5/k_9 + k_5/k_{11}$, the sum of the ratios of the catalytic step to the rate of each unimolecular step in the forward direction (Scheme II). Thus, F26P$_2$ can cause a decrease in $K_{F6P}$ by increasing $k_5$ as long as $C_f$ does not increase by as much as $C_{vf}$. A decrease in the ratio of $C_f/C_{vf}$ due to an increase in $k_5$ would be possible if $C_f$ is essentially zero and $C_{vf}$ is finite, so that

the change in $C_f$ is insignificant compared to the change in $C_{vf}$. It is also possible that a decrease in the off-rate for F6P and an increase in the net rate constant for catalysis both occur. More details concerning the rate of interconversion of the central complexes and the release of FBP are necessary to confirm the effect of $F26P_2$ on the PFK reaction.

*Effects of $Mg^{2+}$ on the PFK-Catalyzed Reaction.* Initial velocity studies at varied $Mg^{2+}$ indicate an activating effect of the metal, giving an increase in the apparent affinity of PFK for MgATP with an increase in $Mg^{2+}$. As with the activator $F26P_2$, the parameter V is not affected by $Mg^{2+}$. Assuming that the rate of the forward reaction is not limited by product release so that V represents the catalytic steps, $Mg^{2+}$ must activate by decreasing the off-rate for MgATP. Although the specific role of $Mg^{2+}$ in decreasing the off-rate for MgATP is uncertain, it is likely that the metal acts at the active site and not an allosteric site, since many enzymes catalyzing phosphoryl transfer reactions have been implicated in having $Mg^{2+}$ as an active site effector (Armstrong *et al.*, 1979; Knight *et al.*, 1984; Sosa *et al.*, 1992; Campos & Beauge, 1992; Bertagnolli & Cook, 1994). The role of a second $Mg^{2+}$ in decreasing the off-rate for MgATP could simply be a structural role in maintaining the proper enzyme conformation, or a chemical role in neutralizing the negative charge(s) on MgATP.

As discussed with the effects of $F26P_2$, it is possible that product release actually does limit the forward reaction rate and masks any $Mg^{2+}$ effect on V. If slow release of products occurs, then it is possible that the $Mg^{2+}$ ion activates by facilitating the catalytic steps, perhaps by stabilizing the transition state. It is likely that $Mg^{2+}$ does indeed have an effect both on the affinity of PFK for MgATP and on the catalytic steps. A proposed mechanism for the activation of PFK by $Mg^{2+}$ is shown in Mechanism II. In the mechanism, the first $Mg^{2+}$ serves to neutralize the negative charge on the $\beta$- and $\gamma$-phosphates of ATP. The second $Mg^{2+}$ increases the affinity for MgATP. In addition, the second $Mg^{2+}$ ion acts as a Lewis acid and neutralizes the negative charge on the $\alpha$-

MECHANISM II.

$Mg^{2+}$ activation mechanism of *Ascaris suum* PFK.

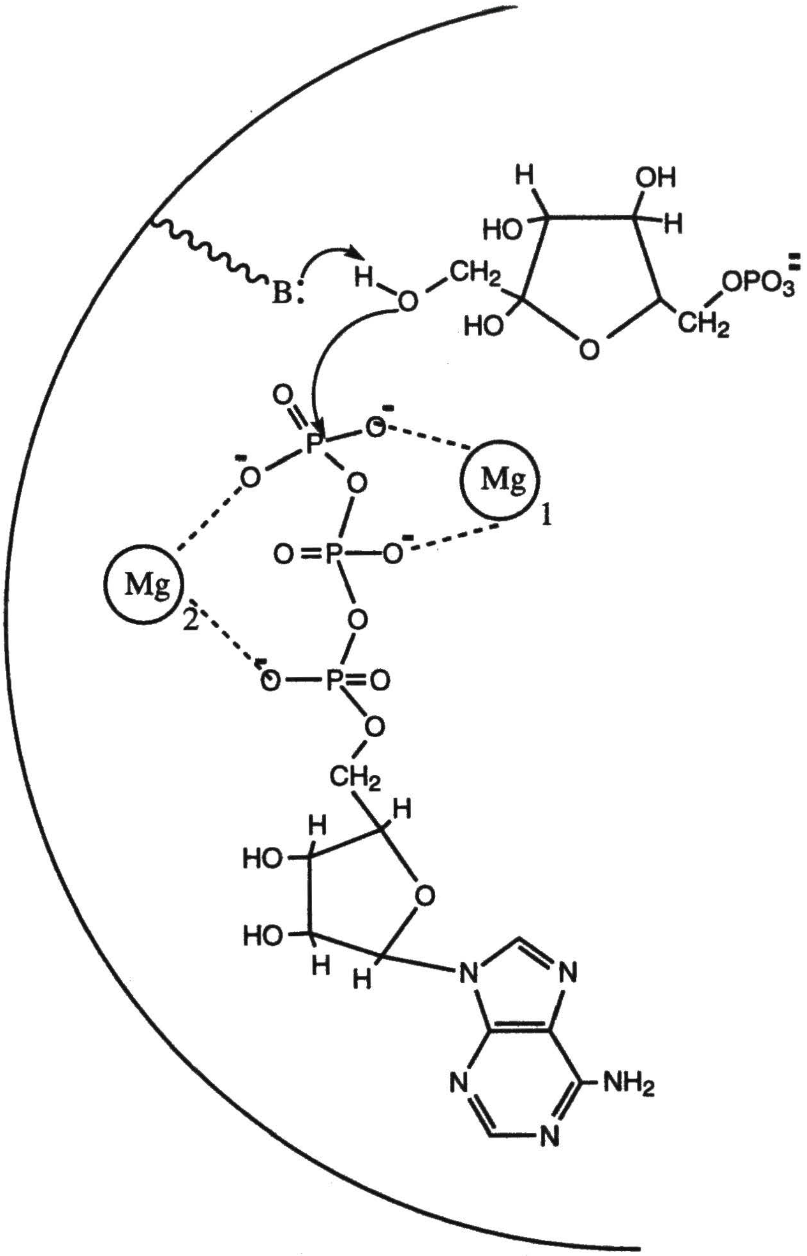
B
H
O
$CH_2$
HO
H
OH
H
HO
O
$OPO_3^{=}$
$CH_2$
P
O
Mg
1
Mg
2
NH₂
N

and/or γ-phosphate of MgATP, thus facilitating nucleophilic attack by the hydroxyl group of F6P.

If $Mg^{2+}$ is an essential activator of *Ascaris suum* PFK, then no activity should occur in its absence. The reaction rate measured in the absence of any added $Mg^{2+}$ is finite (data not shown), being 30% of the rate measured at 10 μM of added $Mg^{2+}$. However, the addition of a micromolar amount of EDTA to the reaction mixture eliminates the activity. The small residual activity is likely to be from contaminating $Mg^{2+}$ in the reaction buffer, since decreasing the concentration of the imidazole reaction buffer from 100 mM to 20 mM causes a decrease in the activity at zero added $Mg^{2+}$. Bertagnolli and Cook (1994) used atomic absorption analysis to show that a background level of as much as 5 μM $Mg^{2+}$ may be present in a reaction mixture similar to the one used in the above-mentioned assays, with most or all of the contaminating $Mg^{2+}$ coming from the buffer. The $Mg^{2+}$ versus MgATP initial velocity pattern (Figure 14) also suggests that a second $Mg^{2+}$ is essential for catalysis. The fit of the equation for a rapid equilibrium ordered binding of substrates and/or effectors to the data indicates that $Mg^{2+}$ must be bound to enzyme before MgATP is able to bind.

The significance of the slight inhibitory effect of $Mg^{2+}$ on *A. suum* PFK at concentrations above 5 mM is uncertain. It is possible that the inhibition is from an ionic strength effect at very high $Mg^{2+}$, either causing a rearrangement of the active site or a change in the charge on active site residues and/or substrates. Another possibility is that the additional metal ion(s) decreases the off-rate of the product MgADP so that at very high $Mg^{2+}$ product release limits the reaction. The catalytic subunit of cyclic AMP-dependent protein kinase has also been shown to be both activated by $Mg^{2+}$ at limiting MgATP, indicated by an increase in $V/K_{MgATP}$, and inhibited at saturating MgATP, indicated by a decrease in V (Cook *et al.*, 1982).

Although the $Mg^{2+}$ activation of PFK activity has been treated as occurring from the binding of a second metal in addition to that bound in the MgATP metal-chelate complex, the actual stoichiometry of $Mg^{2+}$ binding is not known. Indeed, multiple metal ions may be involved in activating the enzyme. Knight *et al.* (1984) showed through nuclear magnetic resonance and electron paramagnetic resonance experiments on the yeast inorganic pyrophosphatase that two divalent cations are necessary at the active site for catalysis to occur in addition to the one divalent cation involved in forming the metal-$PP_i$ complex. Also unknown for the *A. suum* PFK is the physiological significance of $Mg^{2+}$ as an effector of the enzyme. However, the estimated $K_{act}$ for $Mg^{2+}$, 0.4 mM, is within the range of the estimated physiological concentration of $Mg^{2+}$ in *A. suum* muscle tissue (Donahue *et al.*, 1983), suggesting a likely importance. Further studies including atomic absorption, steady-state kinetics, and electron paramagnetic resonance (substituting the paramagnetic $Mn^{2+}$ ion for $Mg^{2+}$) are necessary to elucidate the stoichiometry and chemical role of metal binding with *A. suum* PFK.

*Conclusions.* The data confirm a predominantly steady-state ordered kinetic mechanism for both nPFK and dPFK in the absence of effectors due to the complete trapping of the E:MgATP* complex and no trapping of the putative E:($^{14}$C)F6P complex. It has previously been concluded that dPFK at pH 6.8 exhibits identical characteristics to the native enzyme at pH 8.0. The conformational and/or chemical change that occurs on enzyme upon treatment with DEPC in the presence of F6P is thought to lock the enzyme into an active or 'high-pH' form (Rao *et al.*, 1995). However, the current isotope partitioning and initial velocity data indicate a differential effect of $F26P_2$ on the two enzyme forms. The change from an ordered to a random mechanism in the presence of $F26P_2$ for dPFK but not for nPFK indicates that there must be subtle differences in the dPFK at neutral pH and nPFK at high pH. The data are also consistent with the theory proposed by Payne *et al.* (1995) that $F26P_2$ activates *A. suum* PFK by decreasing the

off-rate for F6P, although more details concerning the rate of release of FBP are necessary to rule out an effect of $F26P_2$ on the catalytic steps. Furthermore, $Mg^{2+}$ has been shown to be an essential activator of *A. suum* PFK. The proposed mechanism involves two divalent metal ions, the first being necessary for the formation of the substrate MgATP and the second being necessary for binding of this substrate to the active site. The second $Mg^{2+}$ also likely plays a role in facilitating the catalytic steps of the reaction. Finally, calculations from the isotope partitioning and initial velocity data as well as the changes seen in the circular dichroic spectra for both nPFK and dPFK indicate that an isomerization occurs upon binding MgATP. The data presented in this dissertation provide the most complete description of the catalytic mechanism of *A. suum* PFK to this date.

# REFERENCES

Armstrong, R. N., Kondo, H., Granot, J., Kaiser, E. T., & Mildvan, A. S. (1979) *Biochemistry* 18, 1230-1238.

Bar-Tana, J., & Cleland, W. W. (1974) *J. Biol. Chem.* 249, 1271-1276.

Bradford, M. M. (1976) *Anal. Biochem.* 72, 248-254.

Bertagnolli, B. L., & Cook, P. F. (1984) *Biochemistry* 23, 4101-4108.

Bertagnolli, B. L., Younathan, E. S., Voll, R. J., & Cook, P. F. (1986) *Biochemistry* 25, 4682-4687.

Bertagnolli, B. L., & Cook, P. F. (1994) *Biochemistry* 33, 1663-1667.

Campos, M., Beauge, L. (1992) *Biochim. Biophys. Acta* 1105, 51-60.

Cheng, T. C. (1986) *General Parasitology,* 2nd ed., 519-521, Academic Press, Inc., Orlando.

Cho, Y. K., Matsunaga, T. O., Kenyon, G. L., Bertagnolli, B. L., & Cook, P. F. (1988) *Biochemistry* 27, 3320-3325.

Claus, T. M., El-Maghrabi, M. R., Regen, D. M., Stewart, H. B., McGrane, M., Kountz, P. D., Nyfeler, F., and Pilkis, S. J. (1984) *Curr. Top. Cell. Regul.* 23, 57-86.

Cleland, W. W. (1979) *Methods Enzymol. 63*, 103-109.

Cook, P. F., Neville, M. E., Jr., Vrana, K. E., Hartl, F. T., & Roskoski, R. Jr. (1982) *Biochemistry* 21, 5794-5799.

Cook, P. F., Rao, Rao, G. S. J., Hofer, H. W., & Harris, B. G. (1987) *J. Biol. Chem.* 262, 14063-14067.

Dann, L. G., & Britton, H. G. (1978) *Biochem. J.* 169, 39.

Dawson, R. M. C., Elliott, D. C., Elliott, W. H., & Jones, K. M. (1986) *Data for Biochemical Research*, 3rd ed., Oxford University Press, New York.

Deville-Bonne, D., Bourgain, F., & Barel, J. (1991) *Biochemistry* 30, 5750-5754.

Donahue, M. J., Yacoub, N. J., Kaeini, M. R., Masaracchia, R. A., & Harris, B. G. (1981) *J. Parasitol.* 67, 505-510.

Donahue, M. J., Masaracchia, R. A., Harris, B. G. (1983) *Mol. Pharmacol.* 23, 378-383.

Fersht, A. (1977) *Enzyme Structure and Mechanism,* pp. 126-127, W. H. Freeman and Co., San Francisco.

Foe, L. G., & Kemp, R. G. (1982) *J. Biol. Chem.* 257, 6368-6372.

Frieden, C., Gilbert, H. R., & Bock, P. E. (1976) *J. Biol. Chem.* 251, 5644-5647.

Gibson, G. E., Harris, B. G., & Cook, P. F. (1996) *Biochemistry* 35,.5451-5457.

Hanson, R. L., Rudolph, F. B., & Lardy, H. A. (1973) *J. Biol. Chem.* 248, 7852-7859.

Hofer, H. W., Allen, B. L., Kaeini, M. R., & Harris, B. G. (1982) *J. Biol. Chem.* 257, 3807-3810.

Kamemoto, E. S., & Mansour, T. E. (1986) *J. Biol. Chem.* 261, 4346-4351.

Kamemoto, E. S., Iltzsch, M. H., Lan, L. & Mansour, T. E. (1987) *Arch. Biochem. Biophys.* 258, 101-111.

Katajima, S., Sakakibara, R., & Uyeda, K. (1983) *J. Biol. Chem.* 258, 1392-1398.

Kee, A., & Griffin, C. C. (1972) *Arch. Biochem. Biophys.* 149, 361-368.

Knight, W. B., Dunaway-Mariano, D., Ransom, S. C., & Villafranca, J. J. (1984) *J. Biol. Chem.* 259, 2886-2890.

Krishnaswamy, P. R., Pamiljans, V., & Meister, A. (1962) *J. Biol. Chem.* 237, 2932.

Kulkarni, G., Rao, G. S. J., Srinivasan, N. G., Hofer, H. W., Yuan, P. M., & Harris, B. G. (1987) *J. Biol. Chem.* 262, 32-34.

Landsperger, W. J., Fodge, D. W., & Harris, B. G. (1978) *J. Biol. Chem.* 253, 1868.

Martell, A. E., & Smith, R. M. (1982) *Critical Stability Constants,* Vol. 5, Plenum Press, New York and London.

Martensen, T. M., & Mansour, T. E. (1976) *J. Biol. Chem.* 251, 3664-3670.

Merry, S., & Britton, H. G. (1985) *Biochem. J.* 226, 13-28.

Mullins, L. S., & Raushel, F. M. (1995) *Methods Enzymol.* 249, 398-425.

Payne, D. M., Powley, D. G., & Harris, B. G. (1979) *J. Parasitol.* 65, 833-841.

Payne, M. A., Rao, G. S. J., Harris, B. G., & Cook, P. F. (1991) *J. Biol. Chem.* 266, 8891-8896.

Payne, M. A., Rao, G. S. J., Harris, B. G., & Cook, P.F. (1995) *Biochemistry* 34, 7781-7787.

Rao, G. S. J., Wariso, B. A., Cook, P.F., Hofer, H. W., & Harris, B. G. (1987a) *J. Biol. Chem.* 262, 14068-14074.

Rao, G. S. J., Harris, B. G., & Cook, P. F. (1987b) *J. Biol. Chem.* 262, 14074-14079.

Rao, G. S. J., Cook, P. F., & Harris, B. G. (1991a) *J. Biol. Chem.* 266, 8884-8890.

Rao, G. S. J., Cook, P. F., & Harris, B. G. (1991b) *Biochemistry* 30, 9998-10004.

Rao, G. S. J., Schnackerz, K. D., Harris, B., G., & Cook, P. F. (1995) *Arch. Bioch. Biophys.* 322, 410-416.

Raushel, R. W., & Cleland, W. W. (1977) *Biochemistry* 16, 2176.

Reinhardt, R. R., Wecker, L., & Cook, P. F. (1984) *J. Biol. Chem.* 259, 7446-7450.

Rose, I. A., O'Connell, E. L., Litwin, S., & Bar-Tana, J. (1974) *J. Biol. Chem.* 249 5163.

Rose, I. A., (1980) *Methods Enzymol.* 64, 47-59.

Saz, H. J., & Lescure, O. L. (1969) *Comp. Biochem. Physiol.* 39, 49-60.

Saz, H. J. (1971) *Am. Zool.* 11, 124-135.

Simon, W. A., & Hofer, H. W., (1978) *Eur. J. Biochem.* 88, 175-181.

Sosa, A., Ordaz, H., Romero, I., Celis, H. (1992) *Biochem. J.* 283, 561-566.

Srinivasan, N. G., Wariso, B. A., Kulkarni, G., Rao, G. S. J., & Harris, B. G. (1988) *J. Biol. Chem.* 263, 3482-3485.

Srinivasan, N. G., Rao, G. S. J., & Harris, B. G. (1990) *Mol. Biochem. Parasitol.* 38, 151-158.

Starling, J. A., Allen, B. L., Payne, D. M., Blytt, H. J. Hofer, H. W., & Harris, B. G. (1982) *J. Biol. Chem.* 257, 3795-3800.

Supowit. S. C., & Harris, B. G. (1976) *Biochim. Biophys. Acta* 422, 48-59.

Thalhofer, H. P., Daum, G., Harris, B. G., & Hofer, H. W. (1988) *J. Biol Chem.* 263, 952-957.

Uyeda, K., Furuya, E., Richard, C. S., & Yokoyama, M. (1982) *Mol. Cell. Biochem.* 48, 97-120.

Uyeda, K. (1979) *Adv. Enzymol. Relat. Areas Mol. Biol.* 48, 193-244.

Uyeda, K. (1970) *J. Biol. Chem.* 245, 2268-2275.

Van Shaftingen, E. (1987) *Adv. Enzymol. Relat. Areas Mol. Biol.* 59, 315-395.

CKMAN
ERY INC.
DEC 96
N. MANCHESTER